



Logistics and Processing Report

GENESIS Airborne Electromagnetic, Magnetic and
Radiometric Geophysical Survey

for

Geological Survey of Ireland

Project Number: AIRJ2621

Acquisition: Sept. 24th, 2014 to Apr. 21st, 2015

Table of contents

1 INTRODUCTION 7

 1.1 Location of the survey area 7

 1.2 General Disclaimer 8

2 SURVEY SPECIFICATIONS AND PARAMETERS 9

 2.1 Survey Area Parameters 9

 2.2 Acquisition System Data Sample Intervals 10

 2.3 Survey specifications 10

 2.4 Survey Tolerances 10

3 SURVEY OPERATIONS 11

 3.1 Aircraft and Geophysical On-Board Equipment 11

 3.2 Navigation System 12

 3.3 Aircraft Magnetometers 12

 3.4 Automatic Compensator / Compensation 12

 3.5 GENESIS Time Domain Electromagnetics 12

 3.6 Radiometric System 14

 3.7 Radar Altitude 14

 3.8 Barometric Pressure Sensor 15

 3.9 Flight Data Recording 15

 3.10 Flight Following 15

 3.11 Magnetic Base Station 15

 3.12 Field Office Equipment 16

 3.13 Survey Personnel 16

4 EQUIPMENT CALIBRATIONS AND DATA ACQUISITION CHECKS 17

 4.1 Survey Calibrations 17

 4.1.1 Dynamic Magnetometer Compensation and Figure of Merit (FOM) 17

 4.1.2 Parallax 17

 4.1.3 Pad Calibrations 18

 4.1.4 Background and Cosmic Calibration Stacks 18

 4.1.5 Height Attenuation Calibrations 18

 4.1.6 Daily Calibrations 18

5 DATA QUALITY CONTROL 19

 5.1 Magnetic Diurnal Data 19

 5.2 Height Data 19

 5.2.1 Radar Altimeter Data 19

 5.2.2 GPS Height Data 19

 5.2.3 Barometric Pressure Data 19

 5.2.4 Topographical Data 19

 5.2.5 Gridding and Inspection 19

 5.3 Flight Path Data 19

 5.4 Magnetic Data 19

5.4.1	Diurnal Correction	20
5.4.2	Parallax Correction	20
5.4.3	Preliminary Gridding and Inspection	20
5.5	GENESIS Data	20
5.5.1	Parallax Correction	20
5.5.2	Preliminary Gridding and Inspection	20
5.6	Spectrometer Data.....	20
5.6.1	Parallax Correction	20
5.6.2	Preliminary Gridding and Inspection	20
5.7	Data Quality Control Results	21
5.7.1	Acquisition Delays.....	21
5.8	Test Line Results	21
6	DATA PROCESSING	22
6.1	Flight Path Recovery	22
6.2	Base Station Diurnal Magnetics.....	22
6.3	Airborne Magnetic Data Processing	22
6.3.1	Magnetic Processing Steps.....	22
6.3.2	Calculated Horizontal Gradients	23
6.3.3	Gridding	23
6.4	GENESIS Data Processing	23
6.4.1	GENESIS Processing Steps	23
6.4.2	Apparent Conductivity	23
6.4.3	Conductivity-Depth-Transforms (CDT).....	23
6.4.4	Gridding	23
6.5	Radiometric Data Processing	24
6.5.1	Radiometric Processing Steps	24
6.5.2	Source Tests.....	24
6.5.3	Gamma-ray Spectrum Stability	24
6.5.4	Spectrometer Resolution Checks.....	24
6.5.5	NASVD Filtering.....	24
6.5.6	Energy Recalibration.....	24
6.5.7	Dead Time	24
6.5.8	STP Altitude	25
6.5.9	Cosmic Aircraft Background Removal	25
6.5.10	Window Definitions	25
6.5.11	Radon Correction.....	26
6.5.12	Spectral Stripping.....	26
6.5.13	Height Correction	27
6.5.14	Conversion to Ground Concentrations.....	27
6.5.15	Gridding	27
6.5.16	Ratio Grids.....	27

6.6	Digital Elevation Model	28
6.6.1	Gridding	28
6.6.2	Disclaimer	28
7	FINAL PRODUCTS	29
7.1	Digital Archives	29
7.2	Report	29
8	APPENDIX I – Data Archive Description	30
8.1	Electromagnetic ASCII and Geosoft Line Archive File Layout (TellusNorth_em.xyz/gdb)	30
8.2	Conductivity Depth Transform ASCII and Geosoft Line Archive File Layout (TellusNorth_cdt.xyz/gdb)	30
8.3	Magnetic ASCII and Geosoft Line Archive File Layout (TellusNorth_mag.xyz/gdb)	31
8.4	Radiometric ASCII and Geosoft Line Archive File Layout (TellusNorth_spec.xyz/gdb)	32
8.5	Radiometric Array Geosoft Line Archive File Layout (TellusNorth_spec_array.gdb)	33
8.6	Radiometric Cesium Geosoft Line Archive File Layout (TellusNorth_spec_cs.gdb)	33
8.7	Grid Archive File description	34
9	APPENDIX II – Grid Products	36
10	APPENDIX III – List of All Supplied Data	49
10.1	Preliminary Gridded Data	49
10.2	Final Located Data	49
10.3	Final Gridded Data	49
10.4	Additional Products	50
11	APPENDIX IV – System Tests and Calibrations	51
11.1	Aircraft VH-ZKB (previously ZS-FSA)	51
11.1.1	Figure of Merit	51
11.1.2	Heading	51
11.1.3	Altimeter Calibration	51
11.1.4	Lag and Parallax Control	51
11.1.5	Pad Calibration	51
11.1.6	Height Attenuation and Sensitivity Calibration	51
11.1.7	Cosmic Test	51
11.1.8	Radon Test	51
11.2	Aircraft VH-ZKG (previously ZS-SSA)	51
11.2.1	Figure of Merit	51
11.2.2	Heading	52
11.2.3	Altimeter Calibration	52
11.2.4	Lag and Parallax Control	52
11.2.5	Pad Calibration	52
11.2.6	Height Attenuation and Sensitivity Calibration	52
11.2.7	Cosmic Test	52
11.2.8	Radon Test	52

Figures

Figure 1: Tellus North Midlands – Location Map.....	7
Figure 2: Survey Aircraft VH-ZKB (previously ZS-FSA).....	12
Figure 3: Magnetic Base Station Locations at Knock Airport.....	16
Figure 4: Magnetic Base Station Locations at Weston Airport.....	16
Figure 5: Tellus North Midlands – Flight Path.....	36
Figure 6: Tellus North Midlands – Terrain (Referenced to Mean Sea Level).....	36
Figure 7: Tellus North Midlands – Residual Magnetic Intensity.....	37
Figure 8: Tellus North Midlands – Total Magnetic Intensity.....	37
Figure 9: Tellus North Midlands – First Vertical Derivative of Total Magnetic Intensity.....	38
Figure 10: Tellus North Midlands – Second Vertical Derivative of Total Magnetic Intensity.....	38
Figure 11: Tellus North Midlands – Calculated Magnetic Lateral Gradient.....	39
Figure 12: Tellus North Midlands – Calculated Magnetic Longitudinal Gradient.....	39
Figure 13: Tellus North Midlands – Total Count (Height Corrected to 60m).....	40
Figure 14: Tellus North Midlands – Potassium (Height Corrected to 60m).....	40
Figure 15: Tellus North Midlands – Thorium (Height Corrected to 60m).....	41
Figure 16: Tellus North Midlands – Uranium (Height Corrected to 60m).....	41
Figure 17: Tellus North Midlands – Total Count Air Absorbed Dose Rate (Using 60m Height Correction).....	42
Figure 18: Tellus North Midlands – Potassium Concentration (Using 60m Height Correction).....	42
Figure 19: Tellus North Midlands – Equivalent Thorium Concentration (Using 60m Height Correction).....	43
Figure 20: Tellus North Midlands – Equivalent Uranium Concentration (Using 60m Height Correction).....	43
Figure 21: Tellus North Midlands – Equivalent Uranium to Percent Potassium Ratio (Using 60m Height Correction).....	44
Figure 22: Tellus North Midlands – Equivalent Uranium to Equivalent Thorium Ratio (Using 60m Height Correction).....	44
Figure 23: Tellus North Midlands – Equivalent Thorium to Percent Potassium Ratio (Using 60m Height Correction).....	45
Figure 24: Tellus North Midlands – Apparent Conductivity Derived from Z-Coil channel 01.....	45
Figure 25: Tellus North Midlands – Apparent Conductivity Derived from Z-Coil channel 02.....	46
Figure 26: Tellus North Midlands – Apparent Conductivity Derived from Z-Coil channel 03.....	46
Figure 27: Tellus North Midlands – Apparent Conductivity Derived from Z-Coil channel 07.....	47
Figure 28: Tellus North Midlands – Conductivity Depth Transform at 0m.....	47
Figure 29: Tellus North Midlands – Conductivity Depth Transform at 25m.....	48
Figure 30: Tellus North Midlands – Conductivity Depth Transform at 50m.....	48

Tables

Table 1: Tellus North Midlands – Survey Boundary Coordinates.....	10
Table 2: Nominal Data Sample Intervals.....	10
Table 3: Tellus North Midlands – Parameters.....	10
Table 4: Survey Tolerances.....	11
Table 5: Survey Aircraft and Equipment.....	11
Table 6: GENESIS Specifications.....	13
Table 7: GENESIS Data Windows.....	13
Table 8: GENESIS waveform and response with gate centres showing positions in sample points.....	14
Table 9: List of Field Office Equipment.....	16
Table 10: Survey Personnel.....	17
Table 11: Parallax Errors.....	18
Table 12: Airborne Data Quality Control Results.....	21
Table 13: Survey Coordinate System.....	22
Table 14: Diurnal Base Values Used.....	22
Table 15: Aircraft Background and Cosmic Stripping Ratio for VH-ZKB (previously ZS-FSA).....	25
Table 16: Aircraft Background and Cosmic Stripping Ratio for VH-ZKG (previously ZS-SSA).....	25
Table 17: Energy Windows requested by the client to match previously flown survey.....	26
Table 18: Radon Stripping Values for VH-ZKB (previously ZS-FSA) and for VH-ZKG (previously ZS-SSA).....	26
Table 19: Stripping Ratios for VH-ZKB (previously ZS-FSA).....	26
Table 20: Stripping Ratios for VH-ZKG (previously ZS-SSA).....	26
Table 21: STP Altitude Coefficients for VH-ZKB (previously ZS-FSA) and for VH-ZKG (previously ZS-SSA).....	27
Table 22: Ground Concentrations for VH-ZKB (previously ZS-FSA) and for VH-ZKG (previously ZS-SSA).....	27

Table 23: Ground Concentrations for VH-ZKB (previously ZS-FSA) and for VH-ZKG (previously ZS-SSA)	27
Table 24: Delivered Reports	29
Table 25: Electromagnetic Data Archive File Layout	30
Table 26: Conductivity Depth Transforms (CDT) Data Archive File Layout	31
Table 27: Magnetic Data Archive File Layout	32
Table 28: Radiometric Data Archive File Layout.....	33
Table 29: Radiometric Array Data Archive File Layout	33
Table 30: Radiometric Cesium Data Archive File Layout.....	34
Table 31: Grid Files	35

1 INTRODUCTION

Between September 24th, 2014 and April 21st, 2015, CGG Airborne Survey (Pty) Ltd. conducted a GENESIS airborne electromagnetic, magnetic and radiometric survey on behalf of the Geological Survey of Ireland, over the Tellus North Midlands area in Ireland.

The survey consisted of one area, flown in 123 flights. Total coverage of the survey area amounted to 32,141 line kilometres. The survey was flown using two Cessna 208B aircraft, registration VH-ZKB (previously ZS-FSA) and VH-ZKG (previously ZS-SSA) owned and operated by CGG. This report summarises the procedures and equipment used by CGG in the acquisition, verification and processing of the airborne geophysical data.

1.1 Location of the survey area

The survey was based out of Knock and Weston Airports, Ireland. The survey aircrafts were operated from the Knock and Weston airports with aircraft fuel available on site. A temporary office was set up in a room at the hotel in Swinford and later at the hotel in Dublin, where all survey operations were run and the initial post flight data verification performed. The survey was based out of Knock Airport from September 24th to October 10th, 2014 and out of Weston Airport from October 10th, 2014 to April 21st, 2015. The base of operation was re-located from Knock Airport to Weston Airport due to regional weather affects which at times impeded production.

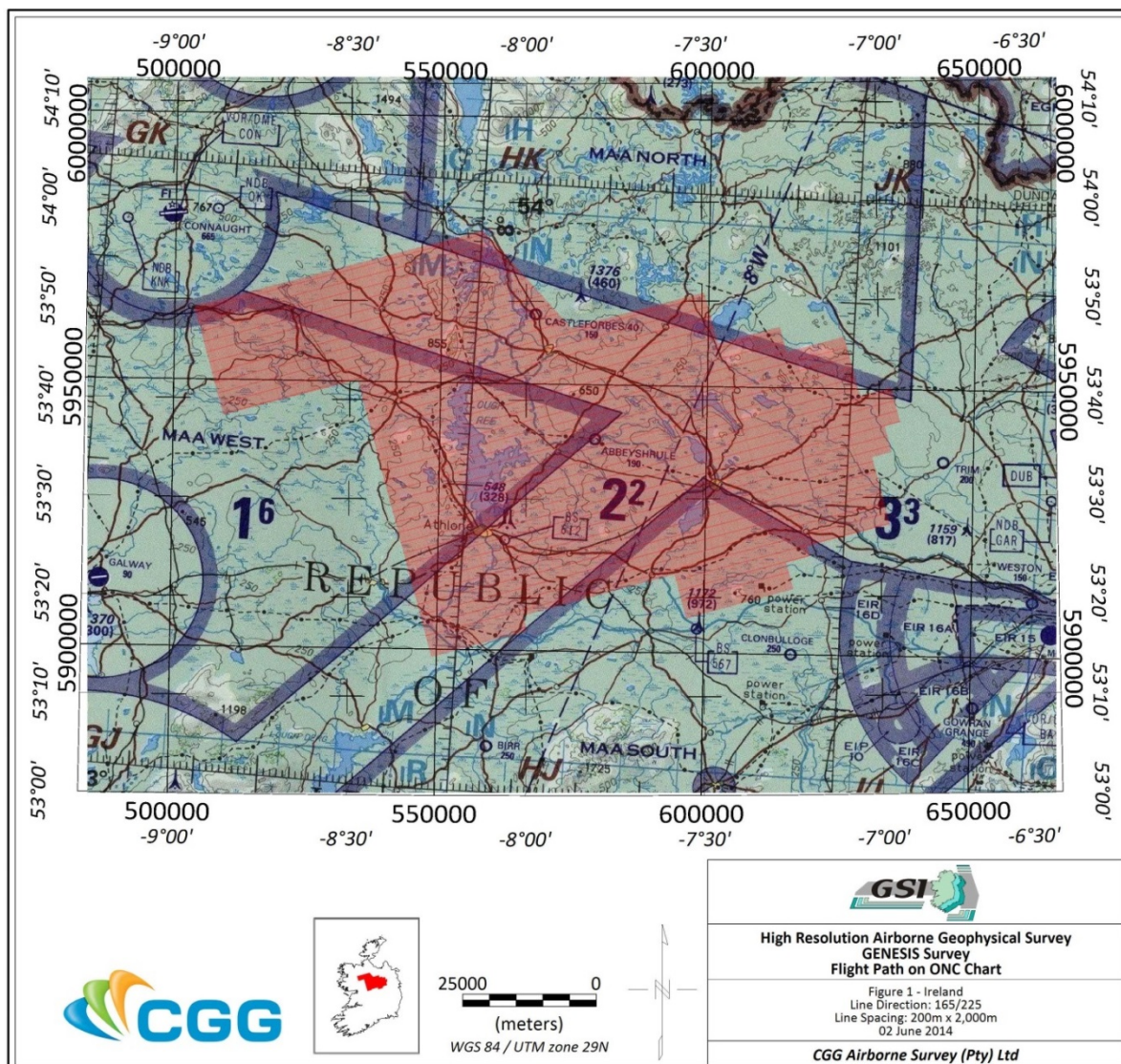


Figure 1: Tellus North Midlands – Location Map

1.2 General Disclaimer

It is CGG's understanding that the data and report provided to the client are to be used for the purpose agreed between the parties. That purpose was a significant factor in determining the scope and level of the Services being offered to the Client. Should the purpose for which the data and report are used change, the data and report may no longer be valid or appropriate and any further use of, or reliance upon, the data and report in those circumstances by the Client without CGG's review and advice shall be at the Client's own and sole risk.

The Services were performed by CGG exclusively for the purposes of the Client. Should the data and report be made available in whole or part to any third party, and such party relies thereon, that party does so wholly at its own and sole risk and CGG disclaims any liability to such party.

Where the Services have involved CGG's use of any information provided by the Client or third parties, upon which CGG was reasonably entitled to rely, then the Services are limited by the accuracy of such information. CGG is not liable for any inaccuracies (including any incompleteness) in the said information, save as otherwise provided in the terms of the contract between the Client and CGG.

2 SURVEY SPECIFICATIONS AND PARAMETERS

2.1 Survey Area Parameters

The survey area is defined by the coordinates in *Table 1*, in UTM Zone 29N projection, referenced to the WGS84 datum.

#	X	Y	Latitude	Longitude
1	503639	5963611	53:49:15.7	-8:56:41.0
2	557500	5978671	53:57:11.5	-8:07:25.6
3	558051	5978070	53:56:51.9	-8:06:55.8
4	558943	5977109	53:56:20.4	-8:06:07.5
5	559529	5976463	53:55:59.3	-8:05:35.8
6	561030	5974859	53:55:06.8	-8:04:14.7
7	562529	5973253	53:54:14.2	-8:02:53.7
8	563424	5972283	53:53:42.4	-8:02:05.4
9	564315	5971316	53:53:10.7	-8:01:17.3
10	565212	5970351	53:52:39.1	-8:00:29.0
11	567012	5968415	53:51:35.6	-7:58:51.9
12	568502	5966802	53:50:42.7	-7:57:31.7
13	569990	5965199	53:49:50.2	-7:56:11.6
14	570893	5964232	53:49:18.4	-7:55:23.0
15	572689	5962298	53:48:15.0	-7:53:46.5
16	573877	5961014	53:47:32.8	-7:52:42.6
17	574277	5960632	53:47:20.3	-7:52:21.1
18	586522	5964068	53:49:04.6	-7:41:08.7
19	599113	5967614	53:50:51.2	-7:29:36.3
20	601947	5958174	53:45:43.9	-7:27:12.5
21	613306	5961356	53:47:18.4	-7:16:48.3
22	614657	5956683	53:44:46.2	-7:15:40.7
23	625385	5959708	53:46:15.1	-7:05:51.0
24	628591	5948667	53:40:15.2	-7:03:12.5
25	634436	5950322	53:41:03.5	-6:57:51.6
26	636172	5944032	53:37:38.4	-6:56:27.0
27	633283	5943149	53:37:12.6	-6:59:05.5
28	634598	5938310	53:34:34.9	-6:58:01.5
29	631024	5937265	53:34:04.3	-7:01:17.3
30	634569	5924790	53:27:17.7	-6:58:24.0
31	619144	5920488	53:25:11.9	-7:12:25.7
32	619723	5918572	53:24:09.5	-7:11:56.9
33	615268	5917295	53:23:31.7	-7:15:59.7
34	616665	5912338	53:20:50.3	-7:14:50.7
35	596764	5906487	53:17:55.5	-7:32:53.0
36	594392	5914710	53:22:23.0	-7:34:52.2

37	566232	5906533	53:18:13.9	-8:00:21.9
38	566548	5905334	53:17:34.9	-8:00:05.7
39	567028	5903711	53:16:42.2	-7:59:41.0
40	549063	5898522	53:14:01.4	-8:15:53.8
41	534385	5950261	53:41:59.7	-8:28:45.0
42	509388	5943358	53:38:20.1	-8:51:28.8

Table 1: Tellus North Midlands – Survey Boundary Coordinates

2.2 Acquisition System Data Sample Intervals

Electromagnetic	~12 m (5 Hz)
Magnetic	~6 m (10 Hz)
Radar Altimeter	~6 m (10 Hz)
Thermometer	~60 m (1 Hz) / ~6 m (10 Hz)
Barometric	~60 m (1 Hz) / ~6 m (10 Hz)
GPS location	~60 m (1 Hz) / ~30 m (2 Hz)
Radiometric	~60 m (1 Hz)
Magnetic Base Station	(2 Hz)

Table 2: Nominal Data Sample Intervals

2.3 Survey specifications

Job Number	2621
Survey Company	CGG
Date Flown	Sept. 24 th , 2014 – Apr. 21 st , 2015
Client	Geological Survey of Ireland
Area Name	Tellus North Midlands, Ireland
Nominal Terrain Clearance	90 m
Traverse Line Spacing	200 m
Traverse Line Direction	165 /345 degrees
Traverse Line Numbers	10010 – 16110
Tie Line Spacing	2000 m
Tie Line Direction	75 / 255 degrees
Tie Line Numbers	18010 – 18420
Total Survey Line Kilometres	32,141 km

Table 3: Tellus North Midlands – Parameters

2.4 Survey Tolerances

As specified in the contract the following tolerances used are shown below in *Table 4*.

Traverse line deviation	Not to exceed +/- 30% of nominated line spacing over 2 km or more.
Tie line deviation	Not to exceed +/- 30% of nominated tie line spacing over 2 km or more.

Terrain clearance deviation	Not to exceed +/-20 m of nominal terrain clearance over 5 km or more, except where such lines breach air regulations, or in the opinion of the pilot, put aircraft and crew at risk.
Total magnetometer system noise	Not to exceed a noise envelope of 0.1 nT.
Magnetic diurnal variation	Non-linear variations not to exceed 12 nT from a long chord of 3 minutes in length or 2nT over any 30 second chord.
GPS quality	PDOP not to exceed 6 and number of Satellites not to be below 4.
Spectrometer resolution and stability	Individual detector resolution and total system survey resolution on the Thorium peak (2615 keV) not to exceed 7%.
Test line radiometric response deviation	Thorium (or other suitable photo peak) response not to deviate by a significant amount from the average response over the duration of the survey.

Table 4: Survey Tolerances

3 SURVEY OPERATIONS

3.1 Aircraft and Geophysical On-Board Equipment

Survey Platform	Cessna 208B
Aircraft Ownership	CGG Airborne Survey (Pty) Ltd.
Aircraft registration	VH-ZKG (previously ZS-SSA) / VH-ZKB (previously ZS-FSA)
Nominal Survey speed	110 knots / 126 mph / 56 m/s
Data Acquisition System	FASDAS
Total Field Magnetometer	Scintrex CS-3 Caesium vapour
Vector Magnetometer	Fluxgate magnetometer
Electromagnetic System	Time-Domain GENESIS system
Gamma-ray Spectrometer	Exploranium GR820 256 Channels
Gamma-ray Detector	10 NaI(Tl) crystals; 33.56 L down, 8.4 L up
Navigation System GPS	CGG Omnistar in VBS (Virtual Base Station) mode Novatel OEM4 GPS receiver
Base Station Magnetometers	2 x Scintrex Caesium vapour
Altimeter	Bendix King KRA-405B
Barometric Pressure Sensor	Vaisala PMB100 Baro Module
Thermometer	Honeywell HIH-4602-A/C
Video Acquisition	Bullet DVR

Table 5: Survey Aircraft and Equipment



Figure 2: Survey Aircraft VH-ZKB (previously ZS-FSA)

3.2 Navigation System

The GPS receiver was integrated as part of the FASDAS system. Navigation displays were generated by the FASDAS software that displayed to the pilot a graphical representation of the line being flown. A pre-defined flight plan, with area boundaries and the start and end of the line co-ordinates, was loaded into memory and used for real-time navigation information. Position co-ordinates and elevation (Referenced to Mean Sea Level) were output and recorded by the acquisition computer.

3.3 Aircraft Magnetometers

The survey was flown using a Scintrex CS-3 ultra-high sensitivity Caesium vapour magnetometer sensor with the sensor mounted in the tail stinger of the aircraft. The sensor provides a Larmor signal that is processed by high precision counters embedded within the FASDAS to provide an operating range of 20,000 to 100,000 nT. The specifications are shown below.

- Nominal Sensitivity: 0.001 nT
- Still Air RMS Noise: 0.05 nT
- Digital Recording Resolution: 0.001 nT
- Magnetic Gradient Tolerance: >20,000 nT/m

3.4 Automatic Compensator / Compensation

The data from the 3-axis fluxgate, were used to post compensate the magnetic data for the effects of the aircraft's motion, i.e. from changes in attitude and heading. The compensation coefficients were calculated from compensation flights carried out before the survey commenced. The compensated output data, with a resolution and sensitivity of 0.001 nT at a sampling rate of 10 times per second, were recorded digitally.

3.5 GENESIS Time Domain Electromagnetics

The GENESIS 3-axis towed bird assembly provides accurate low noise sampling of the X (horizontal in line), Y (horizontal transverse) and Z (vertical) components of the electromagnetic field. The receiver coils measure the time rate of change of the magnetic field (dB/dt). Signals from each axis are transferred to the aircraft through a tow cable specifically designed for its electrical and mechanical properties. Only X and Z data collected were processed and delivered.

Base Frequency	225 Hz
Transmitter Area	134 m ²
Transmitter Turns	1
Waveform	Square Wave (>10 A/μ rise time), with 50% duty cycle
Peak Current	391 A
Peak Moment	52 394Am ²
Average Moment	26 800 Am ²
Sample Rate	153.6 kHz
Samples Per Half Cycle	76.8 kHz
System Bandwidth	Base Frequency to 34 kHz
Flying Height	3D drape
EM Sensor	Towed Bird (3 orthogonal coils, X and Z processed)
Tx-Rx Horizontal Separation	90 m Nominal
Tx-Rx Vertical Separation	43 m Nominal
Stacked Data Output Interval	200 ms
Maximum Number of Output Windows	11 per component

Table 6: GENESIS Specifications

Channel	Start (p)	End (p)	Width (p)	Start (ms)	End (ms)	Width (ms)	Mid (ms)
1	1	1	1	0.000	0.017	0.017	0.009
2	2	2	1	0.017	0.035	0.017	0.026
3	3	4	2	0.035	0.069	0.035	0.052
4	5	7	3	0.069	0.122	0.052	0.095
5	8	11	4	0.122	0.191	0.069	0.156
6	12	17	6	0.191	0.295	0.104	0.243
7	18	25	8	0.295	0.434	0.139	0.365
8	26	38	13	0.434	0.660	0.226	0.547
9	39	58	20	0.660	1.007	0.347	0.833
10	59	87	29	1.007	1.510	0.503	1.259
11	88	127	40	1.510	2.205	0.695	1.858

Table 7: GENESIS Data Windows

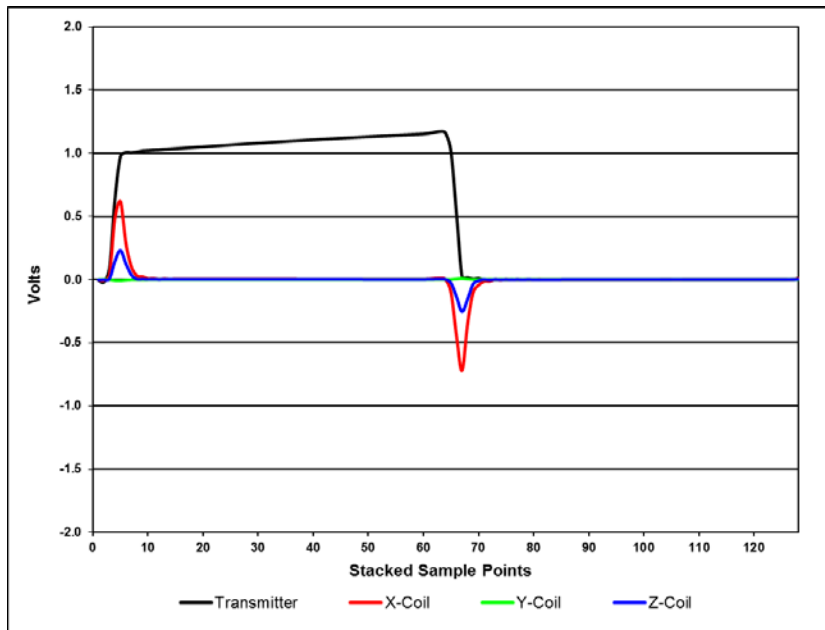


Table 8: GENESIS waveform and response with gate centres showing positions in sample points

3.6 Radiometric System

The radiometric acquisition system consisted of a 256 channel gamma-ray spectrometer and detector system with the following specifications:

- Manufacturer: Exploranium Inc.
- Model: GR-820
- Number of channels: 256
- Crystal Volume: 33.56 L downward looking, 8.4 L upward looking (thermally insulated)
- Sampling interval: 1 s
- Windows (keV):
 - Cesium 137: 648 to 732
 - Potassium: 1368 to 1572
 - Uranium: 1656 to 1860
 - Thorium: 2412 to 2808
 - Total Count: 396 to 2808
 - Cosmic: 4000 to >6000

Data checking of the survey system was carried out by the use of resolution procedures using known radiometric sources. To verify the system, real time displays of individual crystal resolutions and system resolutions, peak channel tracking information, and the energy spectrum showing counts, cosmic level and system dead time were available. The survey system displayed any errors encountered in the spectrometer system.

3.7 Radar Altitude

A Bendix King KRA-405B radio altimeter system was used to measure ground clearance. The radio altimeter indicator provides an absolute altitude display from 0 - 750 metres (0 - 2,500 feet) with a sensitivity of 4 mV/ft. Radar altimeter data were digitally recorded every 0.1 seconds. The specifications are shown below.

- Range: 0 - 2500 ft
- Accuracy: 5%
- Resolution: 4 mV/ft

3.8 Barometric Pressure Sensor

The output of the Vaisala PMB100 Baro Module was used for calculating the barometric altitude of the aircraft. The temperature of the pressure sensor was also recorded. The specifications are shown below.

- Range: Sea level to 10,000 ft
- Accuracy: 5 ft
- Resolution: 1 mV/ft

3.9 Flight Data Recording

All data recorded by the data acquisition system were stored in a digital format on the removable media drive located in the FASDAS. These data were then transferred to the field office computers for post-flight quality control examination. This process was primarily to ensure all the equipment was functioning properly and enables the crew to immediately ascertain that production can resume the following day.

3.10 Flight Following

An integral part of the Safety Management System provides for the installation of a Flight Following System that transmits a position via satellite at pre-determined intervals. The CGG OmniTRACK system is fitted to the aircraft and position information is transmitted every 4 minutes to the Omnistar Network control centre. This information can be monitored by accessing the CGG web page where the updated flight path is displayed. The aircraft is also fitted with an emergency switch and activation of this by the pilot or crew will notify the Omnistar Network control centre immediately. They in turn will contact CGG personnel as per the Emergency Response Plan.

3.11 Magnetic Base Station

Two Scintrex Caesium vapour magnetometers were used to measure the daily variations of the Earth's magnetic field. The base stations were located in an area of low gradient, away from cultural influences. When based at Knock Airport they were positioned approximately 1,100 m apart, approximate co-ordinates (WGS84) of the base stations were as follows, Base A location was 53° 54' 46.0254", -8° 49' 33.8844" and Base B location was 53° 54' 47.4516", -8° 50' 36.3294". When the base of operations was moved to Dublin, the magnetometers were transported to the Weston Airport where they were positioned approximately 200 m apart, approximate co-ordinates (WGS84) of the base stations were as follows, Base A location was 53° 21' 16.5564" -6° 29' 11.6766" and Base B location was 53° 21' 23.6844" -6° 29' 12.1194". They were run continuously throughout the survey flying period with a sampling interval of 1 second at a sensitivity of 0.01 nT. The base station data were closely examined after each day's production flying to determine if any data had been acquired during periods of out-of-specification diurnal variation. In the end Base A was used for final processing of the magnetic data.



Figure 3: Magnetic Base Station Locations at Knock Airport



Figure 4: Magnetic Base Station Locations at Weston Airport

3.12 Field Office Equipment

Computer	High performance laptop -Dell
Printer	Portable printer
DVD writer Drive	Internal DVD+RW format
Hard Drives	Internal hard drives + two external hard drives for redundant backups

Table 9: List of Field Office Equipment

3.13 Survey Personnel

The personnel involved in this project are shown below in *Table 10: Survey Personnel*

Project Supervision - Acquisition	M. Reeve-Fowkes
Project Supervision - Processing	D. Murray
On-site Project Manager	J. Wessels
On-site Crew Leader	J. Wessels
Pilots	M. Reeves, J. Leuschner, G. King, C. Postma, M. Bloemhof, T. Helluege
Aircraft Maintenance Engineer	L. van der Merwe
System Operators	A. van den Berg, D. Strydom, J. Westraat
Data QC and Processing	D. Murray, D. Wilson, K. Zawadzka

Table 10: Survey Personnel

4 EQUIPMENT CALIBRATIONS AND DATA ACQUISITION CHECKS

4.1 Survey Calibrations

A series of calibrations were performed as follows:

4.1.1 Dynamic Magnetometer Compensation and Figure of Merit (FOM)

Carrying a magnetometer through a varying field in a non-uniform orientation produces manoeuvre noise. To compensate for this manoeuvre noise a standard compensation test flight called a “comp box” was flown. The compensation file produced also removed the majority of the heading error. Aircraft compensation tests were flown on the 2 survey line headings.

The data for each heading consists of a series of aircraft manoeuvres with large angular excursions: specifically pitches, rolls and yaws. This was done to artificially create the worst possible attitudes and rates of rotation likely to be encountered while on line and compensate for any magnetic noise created by the aircraft’s motion within the earth’s magnetic field. The data were processed to obtain the real-time compensation terms.

These coefficients were applied in real time or later during post processing if required. Note that this form of compensation will only remove those noise effects modelled in the manoeuvre test flight. Random motions of the stinger with respect to the aircraft airframe generally establish the noise floor for this type of installation.

To verify the effectiveness of the compensation coefficients a second set of manoeuvres were performed that consisted of flying $\pm 10^\circ$ rolls, $\pm 5^\circ$ pitches and $\pm 5^\circ$ yaws peak to peak on headings dictated by the bearing of the traverse and control lines, over periods of 4-5 seconds. A compensation Figure of Merit (FOM) for the aircraft will be calculated by summing up the peak-to-peak amplitudes of the 6 magnetic signatures.

Please refer to Appendix IV for details of the comp boxes and FOMs flown for this survey Appendix II can be found in Appendix V.

4.1.2 Parallax

Parallax error is caused by the physical difference in distance between the various sensors, the electronic delay and software timing in the acquisition system. Hence all variables are subjected to a displacement from the GPS co-ordinates. If these variables are processed without a position offset a parallax error will usually occur. The following corrections were applied for parallax.

Data	Parallax
Radiometrics	0.5 second
GPS	0.0 second
Magnetics	0.3 second
Electromagnetics	2.8 seconds
Radar Altitude	0 second

Table 11: Parallax Errors

4.1.3 Pad Calibrations

A series of tests were taken using a set of radiometric pads of known concentrations of Potassium, Uranium and Thorium. Each crystal pack was tested individually, with data accumulated for 15 minutes. The pad calibration data were processed to determine the radiometric stripping coefficients for each crystal pack. Where aircraft had more than one crystal pack installed, the average of the stripping coefficients were used in final data processing.

4.1.4 Background and Cosmic Calibration Stacks

High-level stacks were flown over the ocean away from the effects of any land based radon. Data were collected for ten minutes at altitudes starting at 8500 feet above sea level and incrementing to 12500 feet above sea level. The high-level stack data were processed to determine the cosmic and aircraft background coefficients.

4.1.5 Height Attenuation Calibrations

Low-level stacks were flown over the Dynamic Calibration Range in Namibia. Data were collected at altitudes above sea level (asl) of 250 ft asl, 340 ft asl, 400 ft asl, 470 ft asl and 540 ft asl, 615 ft asl, 690ft asl, 770 ft asl and 900 ft asl. The neighbouring ocean was flown at the same altitudes, and the data were used as a radon test. These passes alternated between the land and adjacent water sections of the range. A ground survey was carried out on the same day using a calibrated gamma-ray spectrometer.

The airborne and ground data were processed to determine radioelement sensitivity and height attenuation coefficients.

4.1.6 Daily Calibrations

A set of calibrations were performed each survey day as follows:

- Magnetic base station time check
- Spectrometer resolution test
- Low level test line

4.1.6.1 Magnetic Base Station Time Check

At the start of each day all magnetic base stations were time checked and synchronised with the time on the aircraft survey system GPS receiver.

4.1.6.2 Spectrometer Resolution Test

Thorium, Cesium, and Uranium sample checks were performed on the spectrometer before and after each day's survey acquisition. Each sample was placed in a predetermined location and data recorded for 180 sec. Relative count rates above background were within +/- 5% of the average sample checks for the duration of the survey.

5 DATA QUALITY CONTROL

All data QC was conducted at the field office initially, then in Canada for the rest of the survey. At the conclusion of each days survey all magnetic, radiometric, altimeter, flight path and diurnal data were downloaded onto the field office computer for preliminary verification. All raw aircraft data were backed up at the end of each day's survey. One copy was sent to a CGG office in Canada, the other copy remaining at the field office.

5.1 Magnetic Diurnal Data

Diurnal data recorded from the primary base station were checked for spikes and erroneous readings. If invalid diurnal data occurred whilst survey data were being acquired the affected section was re-flown. The diurnal data were also checked to see that the change in diurnal readings during the course of the survey did not exceed the specified tolerances. When this occurred the affected part of the survey line was re-flown. The diurnal data were merged with the aircraft data and used in the verification of the magnetic data.

5.2 Height Data

5.2.1 Radar Altimeter Data

The radar altimeter data were verified to check that a reasonably constant height above the terrain was flown, readings during the course of the survey did not exceed the specified tolerances and for equipment reliability.

5.2.2 GPS Height Data

The aircraft's height above mean sea level each second was determined by real-time differential correction. The GPS height of the aircraft was verified to check for data masking and for equipment reliability.

5.2.3 Barometric Pressure Data

As a backup to the aircraft's GPS height, barometric pressure was also recorded. The barometric pressure of the aircraft was verified to check for equipment reliability. The barometric data were also used in the processing of the radiometric data.

5.2.4 Topographical Data

After verification parallax corrections were applied, the radar altitude was subtracted from the GPS height to give the elevation of the terrain above mean sea level. It was not considered necessary to make any further corrections as this data were for verification purposes only.

5.2.5 Gridding and Inspection

The topographical data were gridded and grid image enhancements were computed and displayed on screen. These were inspected for inconsistencies and errors.

5.3 Flight Path Data

The aircraft's precise location each second was determined by real-time differential correction. The flight path was recovered and plotted daily to ensure it was within specification. Any data not within specification was re-flown. The flight path data was then merged with the rest of the aircraft and diurnal data. Both the aircraft and GPS base station recorded the data in the WGS84 datum.

5.4 Magnetic Data

The raw magnetic data were checked to identify noise and spikes. If the noise exceeded the specified tolerances the part of the line affected was re-flown. After the magnetic data were merged with the digital flight path the following sequence of operations were carried out to allow inspection and verification of the data:

5.4.1 Diurnal Correction

Diurnal base station A was missing for flights 6 to 8, this was addressed by taking the diurnal data from base station B and adjusting it by applying a DC-offset of 50nT for those flights. In addition, diurnal data corresponding to flights 2 - 8 and 506, from base station A, collected at the Knock Airport, was adjusted to match the data corresponding to the rest of the flights collected at the Weston Airport by applying a DC-offset of 140nT. The synchronised digital diurnal data collected by base station A was then filtered to obtain the long wavelength component of the diurnal greater than 71 seconds. This long wavelength component of the diurnal was then subtracted from the corresponding airborne magnetic readings. The base value of 49105 nT was then added back to produce diurnally corrected magnetic data.

5.4.2 Parallax Correction

The diurnally corrected magnetic data were corrected for system parallax using the calculated value.

5.4.3 Preliminary Gridding and Inspection

The magnetic data were gridded and grid image enhancements were computed and displayed on screen. These were inspected for inconsistencies and errors.

5.5 GENESIS Data

The raw electromagnetic data were checked to identify noise and spikes. If the noise exceeded the specified tolerances the part of the line affected was re-flown. After the electromagnetic data were merged with the digital flight path the following sequence of operations were carried out to allow inspection and verification of the data:

5.5.1 Parallax Correction

The electromagnetic data were corrected for system parallax using the calculated value referencing the Z-coil.

5.5.2 Preliminary Gridding and Inspection

The electromagnetic data were gridded and grid image enhancements were computed and displayed on screen. These were inspected for inconsistencies and errors.

5.6 Spectrometer Data

The spectrometer data were verified to check that readings during the course of the survey did not exceed the specified tolerances and for equipment reliability.

5.6.1 Parallax Correction

The raw window data were corrected for system parallax using the calculated value.

5.6.2 Preliminary Gridding and Inspection

The spectrometer data were gridded and grid image enhancements were computed and displayed on screen. These were inspected for inconsistencies and errors.

5.7 Data Quality Control Results

The following data quality related issues have been encountered during the survey.

Base station diurnal magnetic data	None
Airborne magnetic data	None
GENESIS data	No electromagnetic data collected on flights 4 to 8, only tie-lines flown
Data acquisition system	None
Airborne radiometric data	None
Ancillary data	None
Navigation data	None

Table 12: Airborne Data Quality Control Results

5.7.1 Acquisition Delays

Below outlines some of the delays encountered throughout acquisition of the survey:

- Permitting delay with both aircraft in November – 8 days
- Engine replacement with ZH-ZKG (previously ZS-SSA) in November – 21 days
- Christmas Break in December – 10 days
- Registration process with both aircraft in January – 30 days

5.8 Test Line Results

A test line was flown which was referred to as the Bundoran test line with both aircraft VH-ZKB (previously ZS-FSA) and VH-ZKG (previously ZS-SSA) twice throughout the survey, this was used to show repeatability between both aircraft and compared against the previously flown surveys. With VH-ZKB (previously ZS-FSA) the Bundoran test line was flown on December 13th, 2014 and April 16th, 2015, with VH-ZKG (previously ZS-SSA) it was flown on February 19th, 2015 and April 10th, 2015. The test line was approximately 6 kms in length which encompassed both water and land coverage.

6 DATA PROCESSING

6.1 Flight Path Recovery

The aircraft's location for each second was determined by real-time differential correction. These data were recorded in the WGS84 datum.

GPS Recovery:	Real-time differentially corrected GPS.
Projection:	Universal Transverse Mercator (UTM Zone 29N)
Datum:	WGS84
Central meridian:	9° West
False Easting:	500 000 metres
False Northing:	0 metres
Scale factor:	0.9996

Table 13: Survey Coordinate System

6.2 Base Station Diurnal Magnetics

The processing procedures applied to the base station diurnal magnetic data from base station A are summarised below:

- Filter noise by running average filter set to remove wavelengths less than 3 seconds.
- Extract the long wavelength component by running average filter to retain only wavelengths greater than 71 seconds.

6.3 Airborne Magnetic Data Processing

6.3.1 Magnetic Processing Steps

The processing procedures applied to the airborne magnetic data are summarised below:

- Apply any spike corrections to the compensated magnetic variables.
- Interpolate undefined magnetic values.
- Filter diurnal values and subtract them from individual compensated magnetic readings.

Area	Base Value
Tellus North	49105 nT

Table 14: Diurnal Base Values Used

- Apply parallax correction.
- Height correction applied.
- Using the tie lines a set of miss-tie values were determined. These miss-tie values reflected the differences in the magnetic value between the tie lines and the traverse lines over the same geographical point. Using a least squares fit algorithm, which also takes into account the statistical variation inherent in DGPS positioning, a series of corrections were applied to the traverse line data. These allowed the data to be levelled to the same base value.
- A CGG proprietary microlevelling process was applied in order to more subtly level the data.
- Correct for regional effects of the Earth's magnetic field by calculating the IGRF value at each fiducial using IGRF model 2015 and secular variation model.

6.3.2 Calculated Horizontal Gradients

The calculated transverse (lateral) and longitudinal gradients was derived from the residual magnetic intensity grid to enhance the high frequency content of the data and attenuate the low frequency background. It was normalized to nanoteslas per metre based on the cell size.

6.3.3 Gridding

The final levelled magnetic data were gridded using a Minimum Curvature algorithm. Tellus North Midlands was gridded with a cell size of 50 m.

6.4 GENESIS Data Processing

6.4.1 GENESIS Processing Steps

- a) Apply parallax correction.
- b) Apply low order polynomial function through a baseline minimum to correct for drift.
- c) Levelling technique uses statistics of each flight/line and only adjusts if within the predefined threshold specified for each channel by DC corrections.
- d) Height correction

6.4.2 Apparent Conductivity

CGG has developed an algorithm that converts the response in any measurement window into an apparent conductivity. This is performed using a look-up table that contains the response at a range of half-space conductivities and altimeter heights.

The apparent conductivity for the present dataset was calculated using STEP Z-coil channel 01 to 11 inclusive to provide the maximum continuity between the low and high frequency domain data (3 and 12KHZ), when combined with the magnetic signature, provides good geological mapping.

6.4.3 Conductivity-Depth-Transforms (CDT)

The Conductivity-Depth-Transform (CDT) sections were calculated using the Z-coil channels fitted to a layered earth model. The STEP was converted to conductivity as a function of depth, where the structure is assumed to be layers of infinite lateral extent. The features represented in the CDT sections are valid only when these assumptions are met. The electromagnetic method is most sensitive to conductive features so resistive features will be poorly resolved. The process of converting STEP data to conductivity as a function of depth tends to create smoother depth variations than in reality.

The CDT sections, derived from each survey line, are created as individual grids. An additional set of CDT grids have been corrected for altitude variations such that the top of each section reflects the true terrain topography and it is these grids that are displayed on the multi-parameter profiles.

The CDT derived information is also provided in a Geosoft database as an array. The array consists of 41 levels of conductivity, from 0 to 200 metres depth. The conductivity values can be gridded to provide conductivity depth slices for desired depths. On this project, conductivity-depth slices were created for intervals of 0 m, 25 m, 50 m, 75 m, and 100 m depths below the surface.

For more information refer to "Wolfgram P. and Karlik G., 1995: Conductivity-Depth-Transform from MEGATEM data; Exploration Geophysics

6.4.4 Gridding

The final levelled GENESIS data were gridded using a bi-directional spline algorithm. Tellus North Midlands was gridded with a cell size of 50 m.

6.5 Radiometric Data Processing

6.5.1 Radiometric Processing Steps

The radiometric data were processed using the standard IAEA window processing technique as summarised below.

- a) Apply NASVD filtering to the 256 channel radiometric data.
- b) Window the 256 channel data using the IAEA standard energy windows.
- c) Correct for dead time.
- d) Apply spike corrections to the radar altimeter, temperature and pressure values.
- e) Apply parallax corrections to altimeter, temperature and pressure values.
- f) Calculate the equivalent terrain clearance at STP (standard temperature and pressure).
- g) Remove aircraft background.
- h) Remove cosmic background.
- i) Apply stripping ratios and radon correction.
- j) Apply height corrections.
- k) Using the tie lines a set of miss-tie values were determined. These miss-tie values reflected the differences in the value between the tie lines and the traverse lines over the same geographical point. Using a least squares fit algorithm, which also takes into account the statistical variation inherent in DGPS positioning, a series of corrections were applied to the traverse line data. These allowed the data to be levelled to the same base value.
- l) Following this, a CGG proprietary micro-levelling process was applied in order to more subtly level the data.

6.5.2 Source Tests

Thorium source measurements were used daily (before and after flying) to monitor spectrometer sensitivity. Spectrometer energy calibration was performed as part of the source test. This test also detects instrumental problems. Source test data were recorded for the duration of the survey and any significant changes in count rate or individual detector resolution were investigated and resolved. The thorium source test provides primary control over spectrometer function.

6.5.3 Gamma-ray Spectrum Stability

The most effective quality control of spectrometer survey data was achieved by analyzing the 256-channel spectra collected during survey flying. This routine is part of the total quality control measures. Sum spectra for each survey line were created and the potassium and thorium gamma-ray peaks were analyzed for resolution and position.

6.5.4 Spectrometer Resolution Checks

The quality control and monitoring procedures outlined above ensure proper functioning of the spectrometer system, which is critical to AGS. Individual detector resolution and total system survey resolution on the thorium 2615 keV peak were measured and maintained to less than 7%.

6.5.5 NASVD Filtering

The radiometric data were produced with NASVD smoothing. Using the NASVD technique, the raw spectra were first smoothed using 8 principal components. Eigen vectors and statistics on the NASVD processing results were used for analysis.

6.5.6 Energy Recalibration

The spectral drift was checked by monitoring the position of the Potassium, Uranium and Thorium peaks on average spectra along flight lines. The peak positions were determined by using a Gaussian fitting method. Energy recalibration was applied to the spectra using a linear regression (LSQ fit) to determine the slope and intercept. New windowed data were extracted to correct for minor spectral drift.

6.5.7 Dead Time

Gamma-ray spectrometers require a finite time to process each pulse from the detectors. While one pulse is being processed, any other pulse that arrives will be rejected. Consequently the 'live time' of a spectrometer is reduced by the time taken to process all pulses reaching the spectrometer. The spectra are normalised to counts per second by dividing by the live time.

6.5.8 STP Altitude

The radar altimeter data were converted to effective height at standard temperature and pressure using the expression:

$$STPAlt = RAlt \times \frac{P}{1013} \times \frac{273}{(T + 273)}$$

Where:

RAlt = the observed radar altitude in m

T = the measured air temperature in deg. C

P = the barometric pressure in hPa

6.5.9 Cosmic Aircraft Background Removal

The cosmic and aircraft background for each channel are of the form:

$$N = a + b \times C$$

Where:

N = combined cosmic & aircraft background in each spectral window

a = aircraft background in the window

C = cosmic channel count

b = cosmic stripping factor

The aircraft background was removed by subtracting the computed aircraft background from the Total Count, Potassium, Uranium and Thorium windows. The effect of cosmic radiation was removed from each window by multiplying the cosmic channel by the cosmic stripping factor for each window and subtracting the result from the window data.

Window	Aircraft Background	Cosmic Stripping Ratio
Total Count	65.3591	0.6929
Potassium	12.3049	0.0363
Uranium	2.3523	0.0288
Thorium	-0.5398	0.0363
Upward Uranium	0.7197	0.0082

Table 15: Aircraft Background and Cosmic Stripping Ratio for VH-ZKB (previously ZS-FSA)

Window	Aircraft Background	Cosmic Stripping Ratio
Total Count	53.1838	0.6402
Potassium	8.9957	0.0356
Uranium	1.4095	0.0281
Thorium	-0.2924	0.0342
Upward Uranium	0.3067	0.0089

Table 16: Aircraft Background and Cosmic Stripping Ratio for VH-ZKG (previously ZS-SSA)

6.5.10 Window Definitions

The 256 channel data were summed into the standard IAEA windows.

Window	Peak Energy (keV)	Energy Window (keV)		GR-820 Channel Window			
Total Count	-	396	-	2808	33	-	234
Potassium	1470	1368	-	1572	114	-	131
Uranium	1758	1656	-	1860	138	-	155
Thorium	2610	2412	-	2808	201	-	234
Cosmic	-	4000	-	6000		-	
Cesium	690	648	-	732	54	-	61

Table 17: Energy Windows requested by the client to match previously flown survey

6.5.11 Radon Correction

Radon corrections were applied using the upward looking detectors.

Window	Radon Ratios
Total Count	12
Potassium	0.725
Thorium	0.065
Upward Uranium	0.18

Table 18: Radon Stripping Values for VH-ZKB (previously ZS-FSA) and for VH-ZKG (previously ZS-SSA)

The skyshine coefficients a1 and a2 were used to remove any ground-sourced gamma rays that enter the upward looking detector. These were calculated using all the available data. The skyshine coefficients used were 0.03727 and 0.0322, respectively.

6.5.12 Spectral Stripping

Spectral stripping was applied to the Potassium, Uranium, Thorium and Cesium windows. The stripping coefficients were corrected for STP altitude.

Stripping	Value	STP Adjustment (/m)
Alpha	0.2206	0.00049
Beta	0.3973	0.00065
Gamma	0.7074	0.00069
a	0.0444	0
b	-0.0049	0
g	0.0090	0

Table 19: Stripping Ratios for VH-ZKB (previously ZS-FSA)

Stripping	Value	STP Adjustment (/m)
Alpha	0.2467	0.00049
Beta	0.3867	0.00065
Gamma	0.7480	0.00069
a	0.0516	0
b	0.0004	0
g	0.0108	0

Table 20: Stripping Ratios for VH-ZKG (previously ZS-SSA)

6.5.13 Height Correction

The background corrected and stripped window data were corrected for variations in the density altitude of the detector.

Window	Attenuation Coefficient (m^{-1})
Total Count	-0.0076
Potassium	-0.00915
Uranium	-0.0092
Thorium	-0.00796
Cesium	-0.005

Table 21: STP Altitude Coefficients for VH-ZKB (previously ZS-FSA) and for VH-ZKG (previously ZS-SSA)

6.5.14 Conversion to Ground Concentrations

The final height corrected data were converted to the radioelement ground concentrations.

Window	Sensitivity at 60m	Sensitivity at 90m
Total Count	32.1948 cps/nGy/h	25.6278 cps/nGy/h
Potassium	108.7582 cps/%	82.6508 cps/%
Uranium	11.0459 cps/ppm	8.3806 cps/ppm
Thorium	6.0109 cps/ppm	4.7335 cps/ppm
Cesium	0.0144 cps/Bq/m ²	

Table 22: Ground Concentrations for VH-ZKB (previously ZS-FSA) and for VH-ZKG (previously ZS-SSA)

To match a previously flown published data, the sensitivities were adjusted to the following values

Window	Sensitivity at 60m
Total Count	31.6505 cps/nGy/h
Potassium	100.4231 cps/%
Uranium	12.6601 cps/ppm
Thorium	5.377 cps/ppm
Cesium	$(\text{height_corr}+20.8)*414.29-7280$ cps/Bq/m ²

Table 23: Ground Concentrations for VH-ZKB (previously ZS-FSA) and for VH-ZKG (previously ZS-SSA)

6.5.15 Gridding

The final radiometric data were gridded using a minimum curvature algorithm. A grid cell size of 50 m was used for Tellus North Midlands.

6.5.16 Ratio Grids

Ratios of three final radioelement concentrations were calculated, in grid form, using a procedure originally designed by the Geological Survey of Canada GSC. The selected ratios are: thorium-over-potassium; uranium-over-potassium; and uranium-over-thorium. In order to reduce fluctuations caused by limited statistical certainty in the final radioelement concentrations, minimum standards are set for each ratio calculation. These are somewhat arbitrarily selected to equate to a corrected ROI count rate of about 100 c/second for each element. For this spectrometer system these values are:

K	≥ 0.5 %
eU	≥ 0.5 ppm
eTh	≥ 0.5 ppm

Where: K is the concentration of potassium (%)
eU is the equivalent concentration of uranium (ppm)
eTh is the equivalent concentration of thorium (ppm)

Grid points are summed within an expanding search radius around the grid cell, up to the defined maximum, for both the denominator and numerator until the required minima for both are met. If the minima for either the numerator or denominator are not met at the maximum search radius, a null value for the ratio is output.

In order to eliminate calculation of ratios at those locations most likely to be over water, an initial standard is required at each data point before any ratios are calculated. The potassium concentration must be $\geq 0.25\%$. Otherwise all three ratios are set to null. This “kill” process applies only to the initial data point. Such points may be included in the addition process applied to nearby points that have not been “killed”.

6.6 Digital Elevation Model

The processing procedures applied to the terrain data are summarised below:

- a) Apply any spike corrections to the raw radar altimeter data. The radar altimeter was extensively de-spiked due to trees in the survey area.
- b) Interpolate undefined values.
- c) Co-ordinate the data with GPS data.
- d) Apply parallax corrections.
- e) Subtract the aircraft’s height above ground from the aircraft’s height above mean sea level and correct for radar altimeter/GPS sensor separation.

6.6.1 Gridding

The final levelled elevation data were gridded using a bi-directional spline algorithm. A grid cell size of 50 m was used for Tellus North Midlands.

6.6.2 Disclaimer

The accuracy of the elevation calculation is directly dependent on the accuracy of the two input parameters, radar altitude and GPS altitude. The radar altitude value may be erroneous in areas of heavy tree cover, where the altimeter reflects the distance to the tree canopy rather than the ground. The GPS altitude value is primarily dependent on the number of available satellites. Although post-processing of GPS data will yield X and Y accuracies in the order of 1-2 metres, the accuracy of the altitude value is usually much less, sometimes in the ± 5 metre range. Further inaccuracies may be introduced during the interpolation and gridding process.

During this survey the number of active satellites on each flight averaged 9, the average satellite quality was 2, while the horizontal dilution averaged 1.03 with a standard deviation of 0.18.

Because of the inherent inaccuracies of this method, no guarantee is made or implied that the information displayed is a true representation of the height above sea level. Although this product may be of some use as a general reference, **THIS PRODUCT MUST NOT BE USED FOR NAVIGATION PURPOSES.**

7 FINAL PRODUCTS

7.1 Digital Archives

Line and grid data in the form of an ASCII text file (*.xyz), Geosoft database (*.gdb), and Geosoft grids (*.grd) have been written to Hard Drive. The formats and layouts of these archives are further described in in APPENDIX I – Data Archive Description and APPENDIX III – List of All Supplied Data.

7.2 Report

Media/Copies: 1 Digital (Word format)

Table 24: Delivered Reports

8 APPENDIX I – Data Archive Description

8.1 Electromagnetic ASCII and Geosoft Line Archive File Layout (TellusNorth_em.xyz/gdb)

Field	Variable	Description	Units
1	line	Line Number	-
2	flight	Flight Number	-
3	date	Date of Survey Flight	yyyymmdd
4	time	Universal Time (Seconds Since Midnight)	sec
5	heading	Point by Point Bearing	degrees
6	lat_wgs84	Latitude in WGS84	degrees
7	long_wgs84	Longitude in WGS84	degrees
8	x_wgs84	Easting (X) in WGS84 UTM Zone 29N	m
9	y_wgs84	Northing (Y) in WGS84 UTM Zone 29N	m
10	x_itm	Easting (X) in IRENET95 Irish Transverse Mercator	m
11	y_itm	Northing (Y) in IRENET95 Irish Transverse Mercator	m
12	gpsz	GPS Elevation (Referenced to Mean Sea Level)	m
13	alt_radar	Radar Altimeter	m
14	dtm	Terrain (Referenced to Mean Sea Level)	m
15	tx_current	Transmitter Current	A
16	emx_coupling	X-Coil Late Time Normalization Channel	ppm
17	emz_coupling	Z-Coil Late Time Normalization Channel	ppm
18-28	emx_step_raw	Raw X-Coil Channels 01 to 11	ppm
29-39	emz_step_raw	Raw Z-Coil Channels 01 to 11	ppm
40-50	emx_step_final	Levelled X-Coil Channels 01 to 11	ppm
51-61	emz_step_final	Levelled Z-Coil Channels 01 to 11	ppm
62-72	emx_step_hgt	Levelled and Height Corrected X-Coil Channels 01 to 11	ppm
73-83	emz_step_hgt	Levelled and Height Corrected Z-Coil Channels 01 to 11	ppm
84-94	cond_z	Apparent Conductivity Derived from Z-Coil Channels 01 to 11	mS/m
95	depth_0	Conductivity Depth Transform at 0m	mS/m
96	depth_25	Conductivity Depth Transform at 25m	mS/m
97	depth_50	Conductivity Depth Transform at 50m	mS/m
98	depth_75	Conductivity Depth Transform at 75m	mS/m
99	depth_100	Conductivity Depth Transform at 100m	mS/m

Table 25: Electromagnetic Data Archive File Layout

8.2 Conductivity Depth Transform ASCII and Geosoft Line Archive File Layout (TellusNorth_cdt.xyz/gdb)

Field	Variable	Description	Units
1	line	Line Number	-
2	flight	Flight Number	-
3	date	Date of Survey Flight	yyyymmdd

4	time	Universal Time (Seconds Since Midnight)	sec
5	heading	Point by Point Bearing	degrees
6	lat_wgs84	Latitude in WGS84	degrees
7	long_wgs84	Longitude in WGS84	degrees
8	x_wgs84	Easting (X) in WGS84 UTM Zone 29N	m
9	y_wgs84	Northing (Y) in WGS84 UTM Zone 29N	m
10	x_itm	Easting (X) in IRENET95 Irish Transverse Mercator	m
11	y_itm	Northing (Y) in IRENET95 Irish Transverse Mercator	m
12	gpsz	GPS Elevation (Referenced to Mean Sea Level)	m
13	alt_radar	Radar Altimeter	m
14	dtm	Terrain (Referenced to Mean Sea Level)	m
15-55	cond	Conductivity at Depth Below Surface from 0 - 200m at 5 m Intervals	mS/m
56-96	depth	Depth Below Surface (0 - 200m)	m

Table 26: Conductivity Depth Transforms (CDT) Data Archive File Layout

8.3 Magnetic ASCII and Geosoft Line Archive File Layout (TellusNorth_mag.xyz/gdb)

Field	Variable	Description	Units
1	line	Line Number	-
2	flight	Flight Number	-
3	date	Date of Survey Flight	yyyymmdd
4	time	Universal Time (Seconds Since Midnight)	sec
5	heading	Point by Point Bearing	degrees
6	lat_wgs84	Latitude in WGS84	degrees
7	long_wgs84	Longitude in WGS84	degrees
8	x_wgs84	Easting (X) in WGS84 UTM Zone 29N	m
9	y_wgs84	Northing (Y) in WGS84 UTM Zone 29N	m
10	x_itm	Easting (X) in IRENET95 Irish Transverse Mercator	m
11	y_itm	Northing (Y) in IRENET95 Irish Transverse Mercator	m
12	gpsz	GPS Elevation (Referenced to Mean Sea Level)	m
13	alt_radar	Radar Altimeter	m
14	dtm	Terrain (Referenced to Mean Sea Level)	m
15	drape	Drape Flying Surface (Referenced to Mean Sea Level)	m
16	diurnalA	Magnetic Ground Base Station (Used for Levelling)	nT
17	diurnalB	Magnetic Ground Base Station	nT
18	mag_port_raw	Total Magnetic Intensity (Uncompensated) from the Port Wingtip Sensor	nT
19	mag_port_comp	Total Magnetic Intensity (Compensated) from the Port Wingtip Sensor	nT
20	mag_port_tmi	Total Magnetic Intensity (Levelled) from the Port Wingtip Sensor	nT
21	mag_port_rmi	Residual Magnetic Intensity (Levelled) from the Port Wingtip Sensor	nT
22	mag_star_raw	Total Magnetic Intensity (Uncompensated) from the Starboard Wingtip Sensor	nT
23	mag_star_comp	Total Magnetic Intensity (Compensated) from the Starboard Wingtip Sensor	nT
24	mag_star_tmi	Total Magnetic Intensity (Levelled) from the Starboard Wingtip Sensor	nT
25	mag_star_rmi	Residual Magnetic Intensity (Levelled) from the Starboard Wingtip Sensor	nT

26	igrf	International Geomagnetic Reference Field	nT
27	gradlat_calc	Calculated Lateral Horizontal Magnetic Gradient (Levelled) from the Starboard Wingtip Sensor	nT/m
28	gradlong_calc	Calculated Longitudinal Horizontal Magnetic Gradient (Levelled) from the Starboard Wingtip Sensor	nT/m

Table 27: Magnetic Data Archive File Layout

8.4 Radiometric ASCII and Geosoft Line Archive File Layout (TellusNorth_spec.xyz/gdb)

Field	Variable	Description	Units
1	line	Line Number	-
2	flight	Flight Number	-
3	date	Date of Survey Flight	yyyymmdd
4	time	Universal Time (Seconds Since Midnight)	sec
5	heading	Point by Point Bearing	degrees
6	lat_wgs84	Latitude in WGS84	degrees
7	long_wgs84	Longitude in WGS84	degrees
8	x_wgs84	Easting (X) in WGS84 UTM Zone 29N	m
9	y_wgs84	Northing (Y) in WGS84 UTM Zone 29N	m
10	x_itm	Easting (X) in IRENET95 Irish Transverse Mercator	m
11	y_itm	Northing (Y) in IRENET95 Irish Transverse Mercator	m
12	gpsz	GPS Elevation (Referenced to Mean Sea Level)	m
13	alt_radar	Radar Altimeter	m
14	dtm	Terrain (Referenced to Mean Sea Level)	m
15	pres	Air Pressure	kPa
16	temp	Air Temperature	degrees Celcius
17	alt_stp	Standard Temperature and Pressure Altitude	m
18	livetime	Spectrometer Live Time	ms
19	tc_raw	Total Count Raw	cps
20	k_raw	Potassium Count Raw	cps
21	u_raw	Uranium Count Raw	cps
22	th_raw	Thorium Count Raw	cps
23	u_up_raw	Upward Uranium Count Raw	cps
24	cosmic	Cosmic Count Raw	cps
25	radon	Filtered Radon	cps
26	tc_60	Height Corrected Total Count (60m)	cps
27	k_60	Height Corrected Potassium Count (60m)	cps
28	u_60	Height Corrected Uranium Count (60m)	cps
29	th_60	Height Corrected Thorium Count (60m)	cps
30	tc_90	Height Corrected Total Count (90m)	cps
31	k_90	Height Corrected Potassium Count (90m)	cps
32	u_90	Height Corrected Uranium Count (90m)	cps
33	th_90	Height Corrected Thorium Count (90m)	cps

34	tc_dose	Total Count Air Absorbed Dose Rate (Using 60m Height Correction)	nGy/h
35	kconc	Percent Potassium (Using 60m Height Correction)	%
36	eu	Equivalent Uranium Concentration (Using 60m Height Correction)	ppm
37	eth	Equivalent Thorium Concentration (Using 60m Height Correction)	ppm

Table 28: Radiometric Data Archive File Layout

8.5 Radiometric Array Geosoft Line Archive File Layout (TellusNorth_spec_array.gdb)

Variable	Description	Units
line	Line Number	-
flight	Flight Number	-
date	Date of Survey Flight	yyyymmdd
time	Universal Time (Seconds Since Midnight)	sec
heading	Point by Point Bearing	degrees
lat_wgs84	Latitude in WGS84	degrees
long_wgs84	Longitude in WGS84	degrees
x_wgs84	Easting (X) in WGS84 UTM Zone 29N	m
y_wgs84	Northing (Y) in WGS84 UTM Zone 29N	m
x_itm	Easting (X) in IRENET95 Irish Transverse Mercator	m
y_itm	Northing (Y) in IRENET95 Irish Transverse Mercator	m
gpsz	GPS Elevation (Referenced to Mean Sea Level)	m
alt_radar	Radar Altimeter	m
dtm	Terrain (Referenced to Mean Sea Level)	m
pres	Air Pressure	kPa
temp	Air Temperature	degrees Celcius
alt_stp	Standard Temperature and Pressure Altitude	m
lifetime	Spectrometer Live Time	ms
cosmic	Cosmic Count Raw	cps
spec256_down	Raw Downward Looking Radiometric Spectra	cps
spec256_up	Raw Upward Looking Radiometric Spectra	cps
spec256_down_nas	NASVD Downward Looking Radiometric Spectra	cps
spec256_up_nas	NASVD Upward Looking Radiometric Spectra	cps

Table 29: Radiometric Array Data Archive File Layout

8.6 Radiometric Cesium Geosoft Line Archive File Layout (TellusNorth_spec_cs.gdb)

Field	Variable	Description	Units
1	line	Line Number	-
2	flight	Flight Number	-
3	date	Date of Survey Flight	yyyymmdd
4	time	Universal Time (Seconds Since Midnight)	sec
5	heading	Point by Point Bearing	degrees
6	lat_wgs84	Latitude in WGS84	degrees

7	long_wgs84	Longitude in WGS84	degrees
8	x_wgs84	Easting (X) in WGS84 UTM Zone 29N	m
9	y_wgs84	Northing (Y) in WGS84 UTM Zone 29N	m
10	x_itm	Easting (X) in IRENET95 Irish Transverse Mercator	m
11	y_itm	Northing (Y) in IRENET95 Irish Transverse Mercator	m
12	gpsz	GPS Elevation (Referenced to Mean Sea Level)	m
13	alt_radar	Radar Altimeter	m
14	dtm	Terrain (Referenced to Mean Sea Level)	m
15	pres	Air Pressure	kPa
16	temp	Air Temperature	degrees Celcius
17	alt_stp	Standard Temperature and Pressure Altitude	m
18	livetime	Spectrometer Live Time	ms
19	cosmic	Cosmic Count Raw	cps
20	radon	Filtered Radon	cps
21	cs_att_60	Height Corrected Cesium 137 Count (60m)	cps
22	cs_con	Cesium 137	Bq/m ²
23	cs_con_ml	Filtered Cesium 137	Bq/m ²

Table 30: Radiometric Cesium Data Archive File Layout

8.7 Grid Archive File description

The grids are in Geosoft format. A grid cell size of 50 m was used for all area grids.

File	Description	Units
TellusNorth_dtm.grd	Terrain (Referenced to Mean Sea Level)	m
TellusNorth_(Sensor)_rmi.grd	Residual Magnetic Intensity	nT
TellusNorth_(Sensor)_tmi.grd	Total Magnetic Intensity	nT
TellusNorth_(Sensor)_vd1.grd	First Vertical Derivative of Total Magnetic Intensity	nT/m
TellusNorth_(Sensor)_vd2.grd	Second Vertical Derivative of Total Magnetic Intensity	nT/m ²
TellusNorth_(Sensor)_gradlat_calc.grd	Calculated Magnetic Lateral Gradient of Total Magnetic Intensity	nT/m
TellusNorth_(Sensor)_gradlong_calc.grd	Calculated Magnetic Longitudinal Gradient of Total Magnetic Intensity	nT/m
TellusNorth_tc_60.grd	Total Count (Height Corrected to 60m)	cps
TellusNorth_k_60.grd	Potassium (Height Corrected to 60m)	cps
TellusNorth_th_60.grd	Thorium (Height Corrected to 60m)	cps
TellusNorth_u_60.grd	Uranium (Height Corrected to 60m)	cps
TellusNorth_tc_90.grd	Total Count (Height Corrected to 90m)	cps
TellusNorth_k_90.grd	Potassium (Height Corrected to 90m)	cps
TellusNorth_th_90.grd	Thorium (Height Corrected to 90m)	cps
TellusNorth_u_90.grd	Uranium (Height Corrected to 90m)	cps
TellusNorth_tc_dose.grd	Total Count Air Absorbed Dose Rate (Using 60m Height Correction)	nGy/h
TellusNorth_kconc.grd	Potassium Concentration (Using 60m Height Correction)	%
TellusNorth_eth.grd	Equivalent Thorium Concentration(Using 60m Height Correction)	ppm
TellusNorth_eu.grd	Equivalent Uranium Concentration (Using 60m Height Correction)	ppm

TellusNorth_ratio_u_k	Equivalent Uranium to Percent Potassium Ratio (Using 60m Height Correction)	ppm/%
TellusNorth_ratio_u_th	Equivalent Uranium to Equivalent Thorium Ratio (Using 60m Height Correction)	-
TellusNorth_ratio_th_k	Equivalent Thorium to Percent Potassium Ratio (Using 60m Height Correction)	ppm/%
TellusNorth_cond_z01.grd	Apparent Conductivity Derived from Z-Coil channel 01	mS/m
TellusNorth_cond_z02.grd	Apparent Conductivity Derived from Z-Coil channel 02	mS/m
TellusNorth_cond_z03.grd	Apparent Conductivity Derived from Z-Coil channel 03	mS/m
TellusNorth_cond_z04.grd	Apparent Conductivity Derived from Z-Coil channel 04	mS/m
TellusNorth_cond_z05.grd	Apparent Conductivity Derived from Z-Coil channel 05	mS/m
TellusNorth_cond_z06.grd	Apparent Conductivity Derived from Z-Coil channel 06	mS/m
TellusNorth_cond_z07.grd	Apparent Conductivity Derived from Z-Coil channel 07	mS/m
TellusNorth_cond_z08.grd	Apparent Conductivity Derived from Z-Coil channel 08	mS/m
TellusNorth_cond_z09.grd	Apparent Conductivity Derived from Z-Coil channel 09	mS/m
TellusNorth_cond_z10.grd	Apparent Conductivity Derived from Z-Coil channel 10	mS/m
TellusNorth_cond_z11.grd	Apparent Conductivity Derived from Z-Coil channel 11	mS/m
TellusNorth_depth_0m.grd	Conductivity Depth Transform at 0m	mS/m
TellusNorth_depth_25m.grd	Conductivity Depth Transform at 25m	mS/m
TellusNorth_depth_50m.grd	Conductivity Depth Transform at 50m	mS/m
TellusNorth_depth_75m.grd	Conductivity Depth Transform at 75m	mS/m
TellusNorth_depth_100m.grd	Conductivity Depth Transform at 100m	mS/m

Table 31: Grid Files

9 APPENDIX II – Grid Products

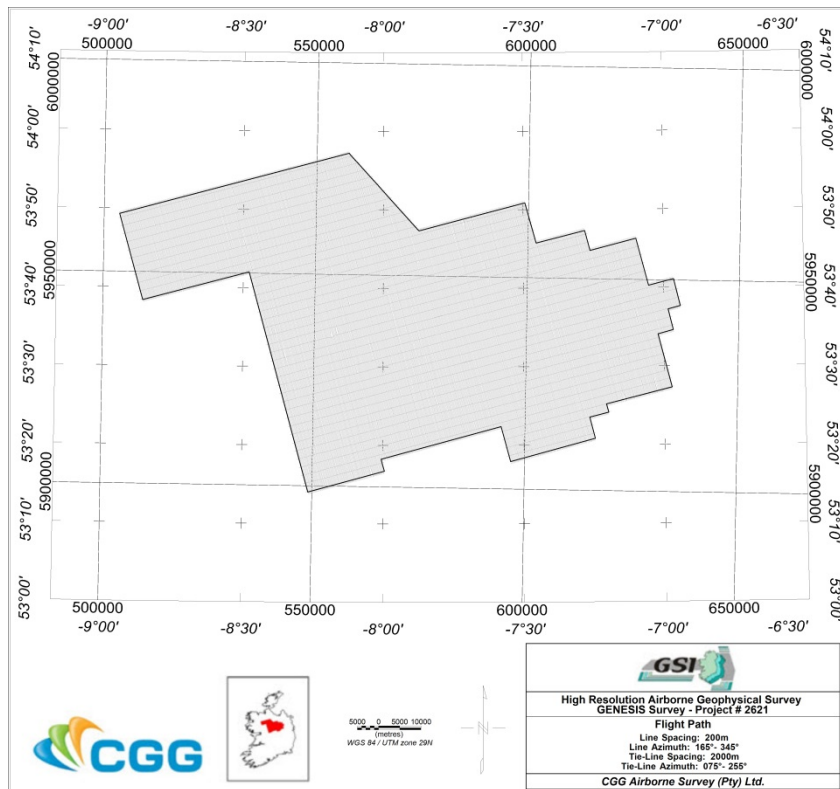


Figure 5: Tellus North Midlands – Flight Path

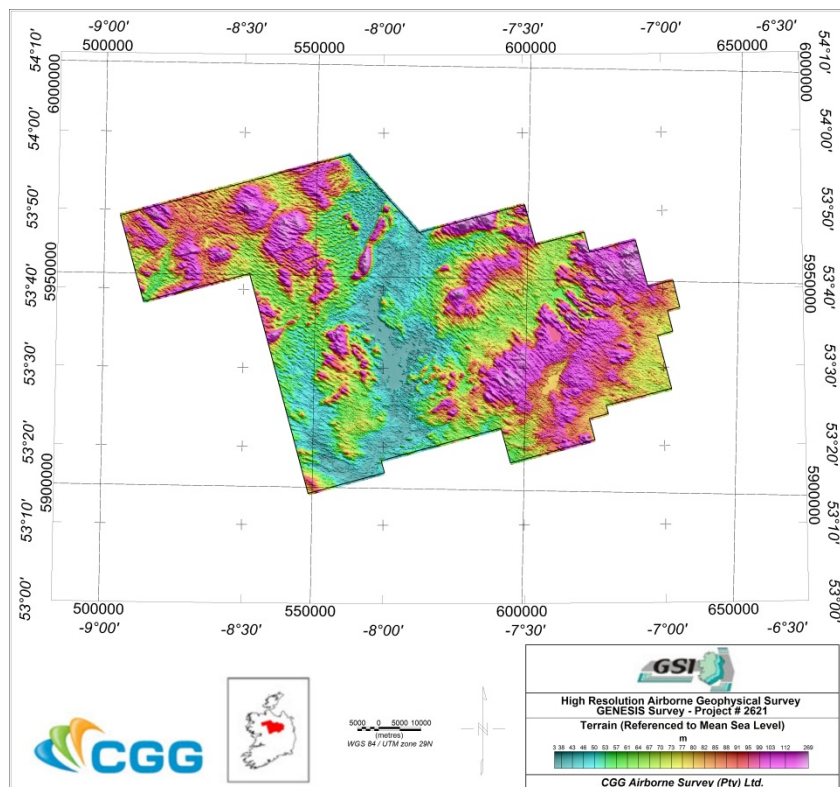


Figure 6: Tellus North Midlands – Terrain (Referenced to Mean Sea Level)

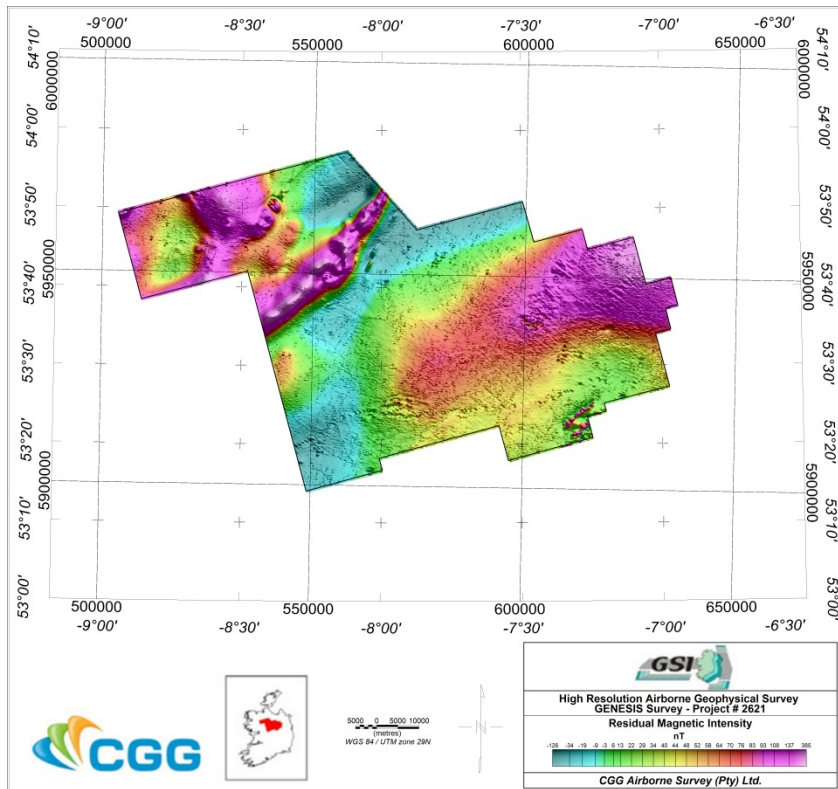


Figure 7: Tellus North Midlands – Residual Magnetic Intensity

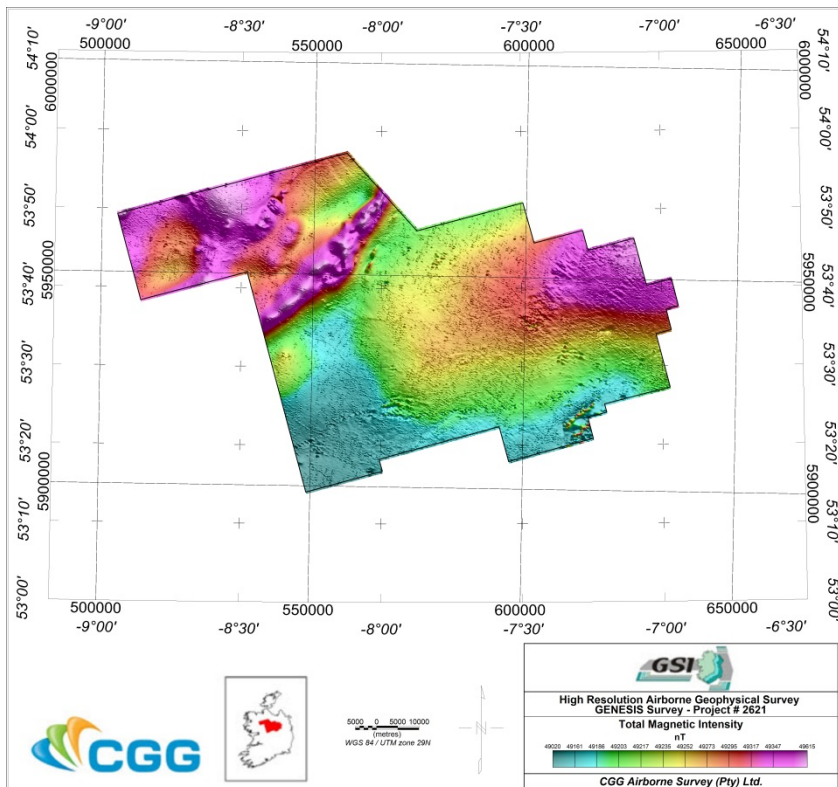


Figure 8: Tellus North Midlands – Total Magnetic Intensity

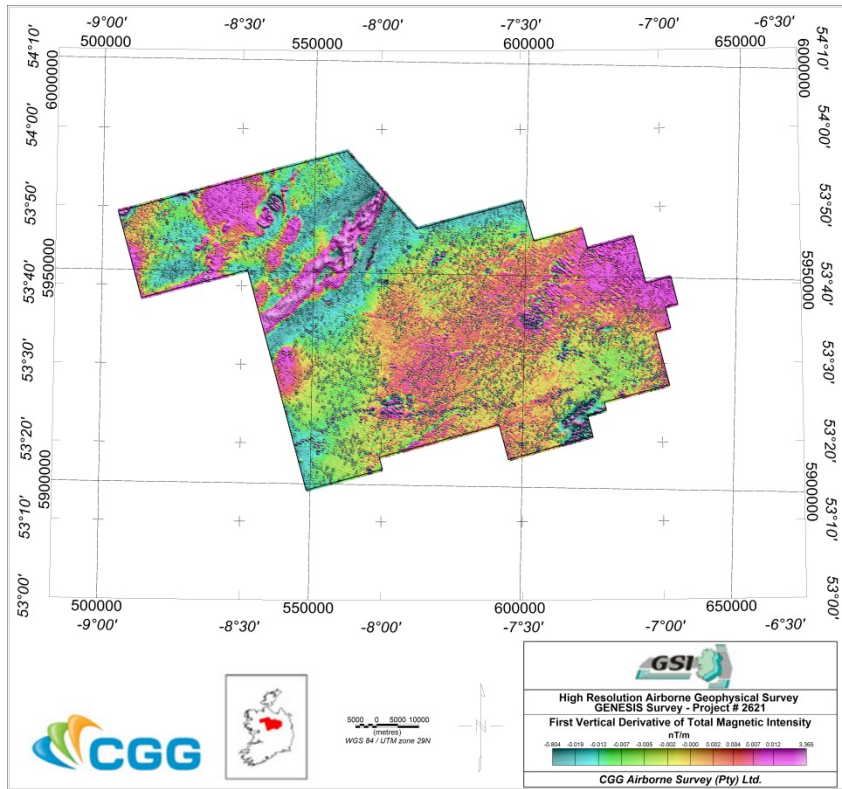


Figure 9: Tellus North Midlands – First Vertical Derivative of Total Magnetic Intensity

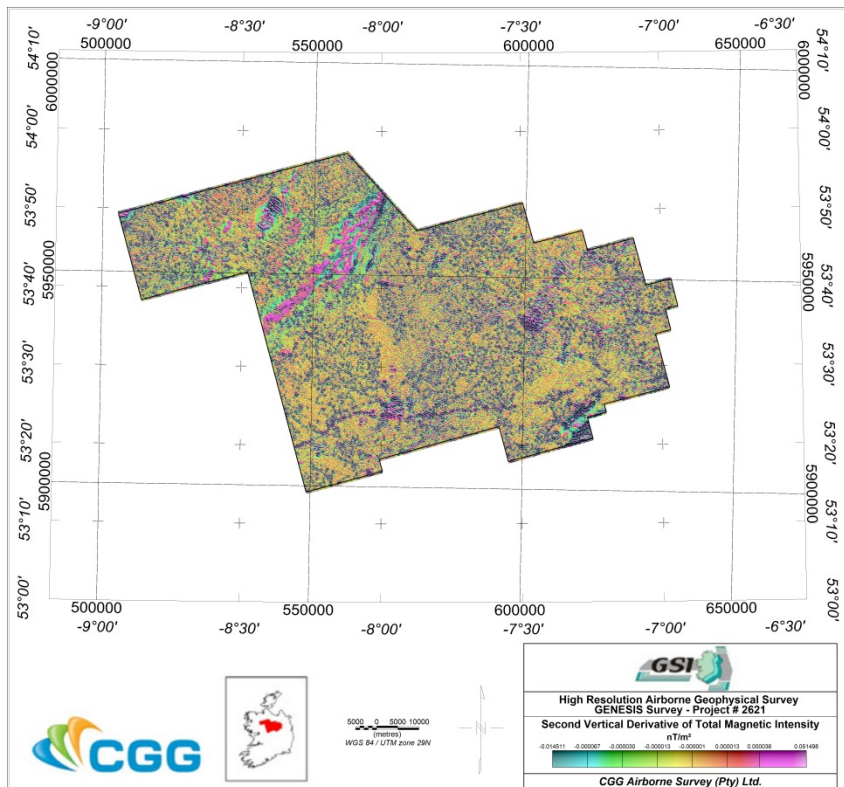


Figure 10: Tellus North Midlands – Second Vertical Derivative of Total Magnetic Intensity

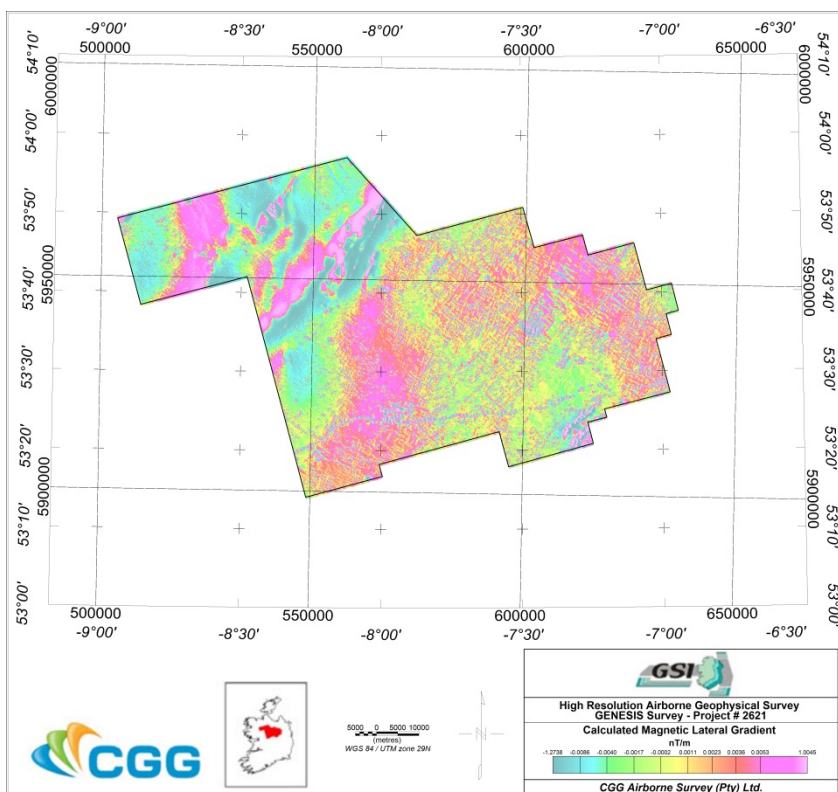


Figure 11: Tellus North Midlands – Calculated Magnetic Lateral Gradient

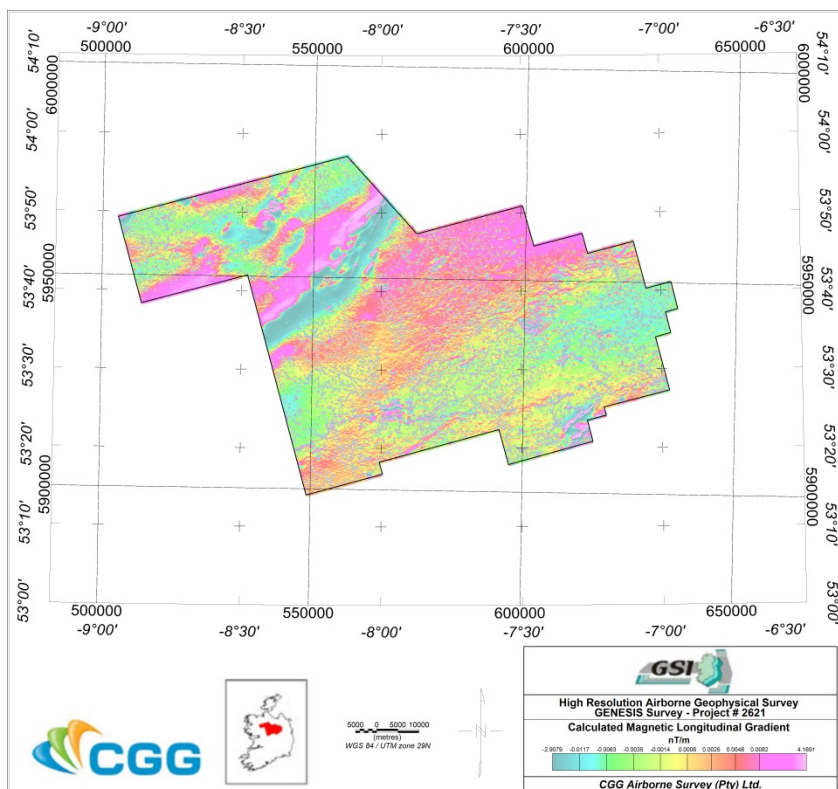


Figure 12: Tellus North Midlands – Calculated Magnetic Longitudinal Gradient

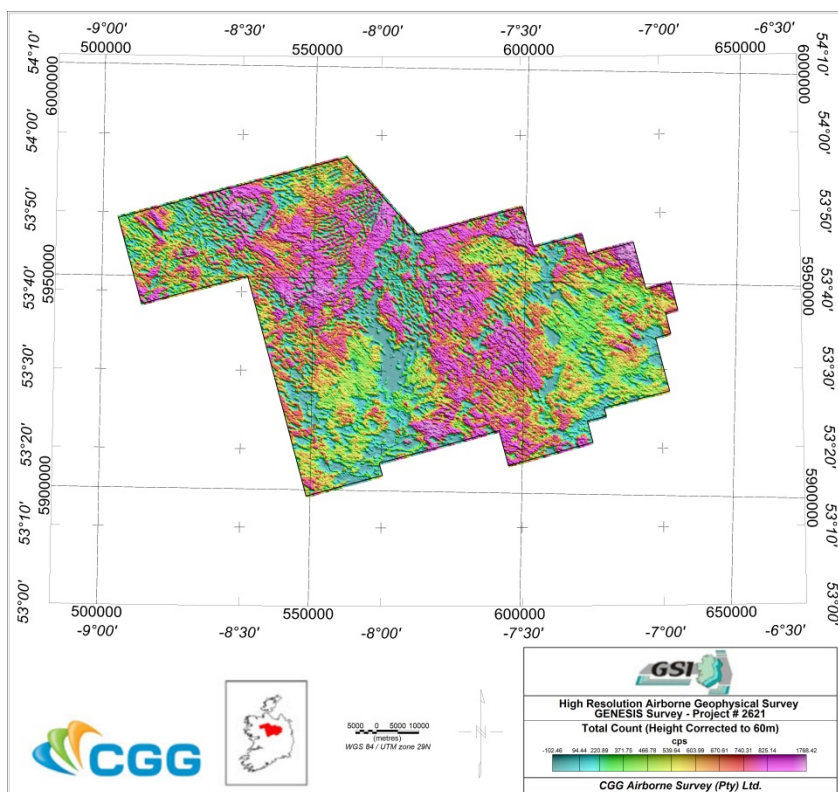


Figure 13: Tellus North Midlands – Total Count (Height Corrected to 60m)

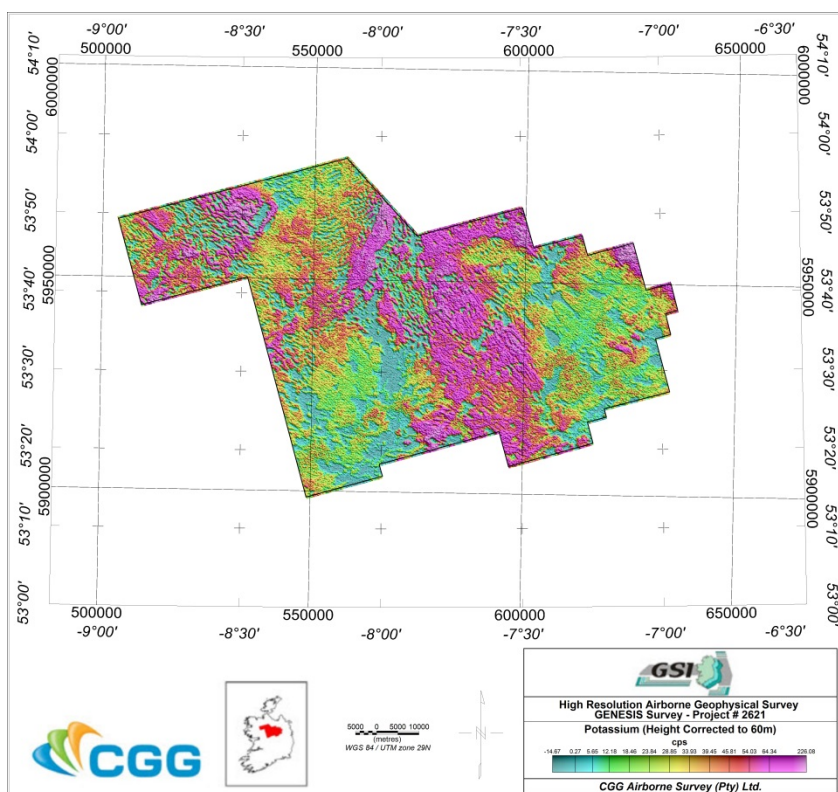


Figure 14: Tellus North Midlands – Potassium (Height Corrected to 60m)

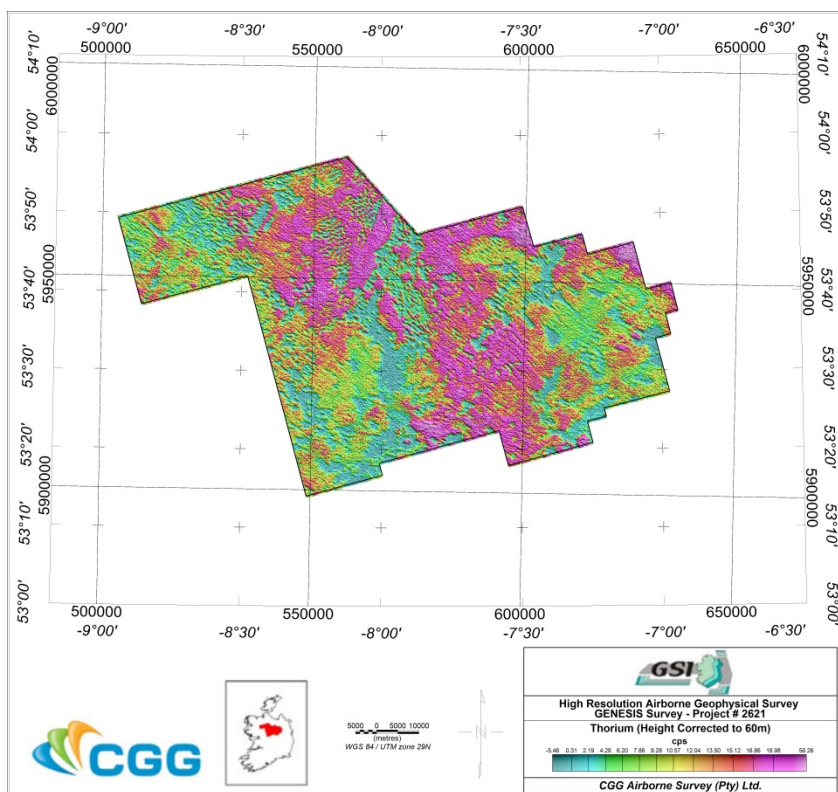


Figure 15: Tellus North Midlands – Thorium (Height Corrected to 60m)

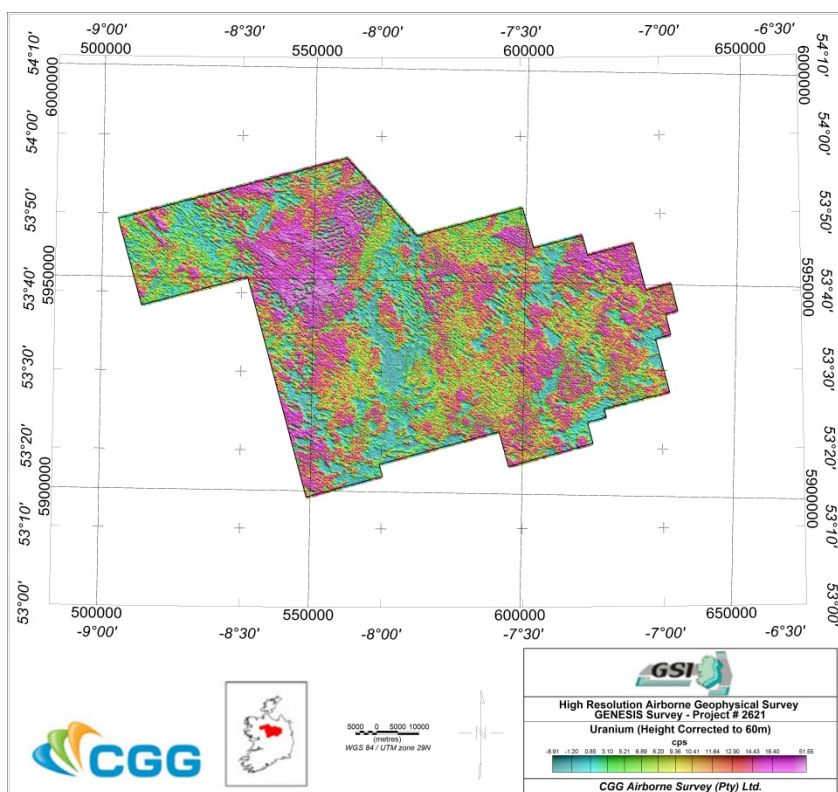


Figure 16: Tellus North Midlands – Uranium (Height Corrected to 60m)

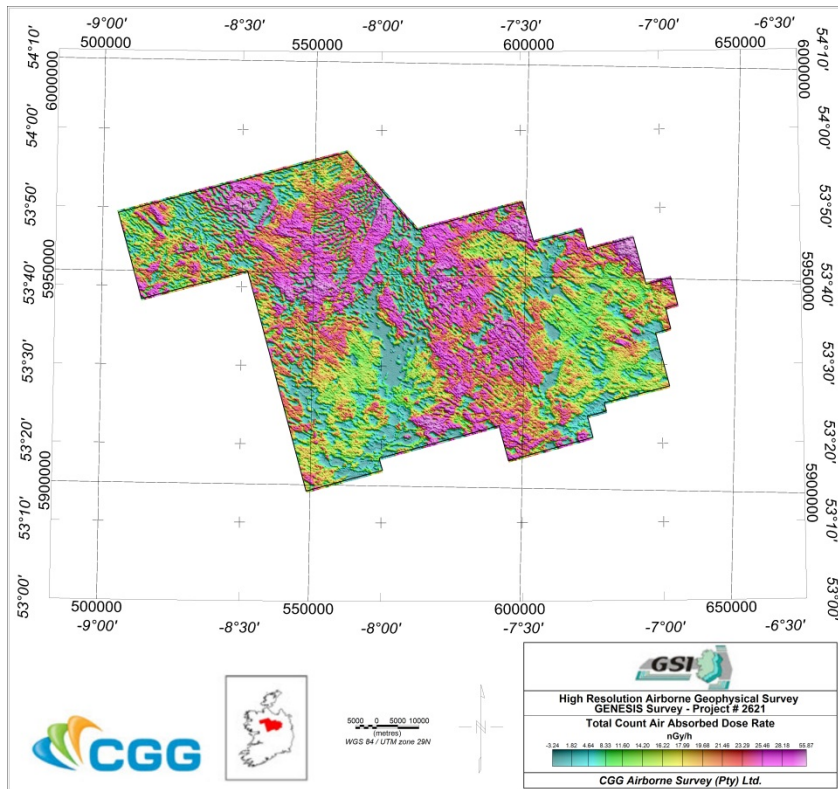


Figure 17: Tellus North Midlands – Total Count Air Absorbed Dose Rate (Using 60m Height Correction)

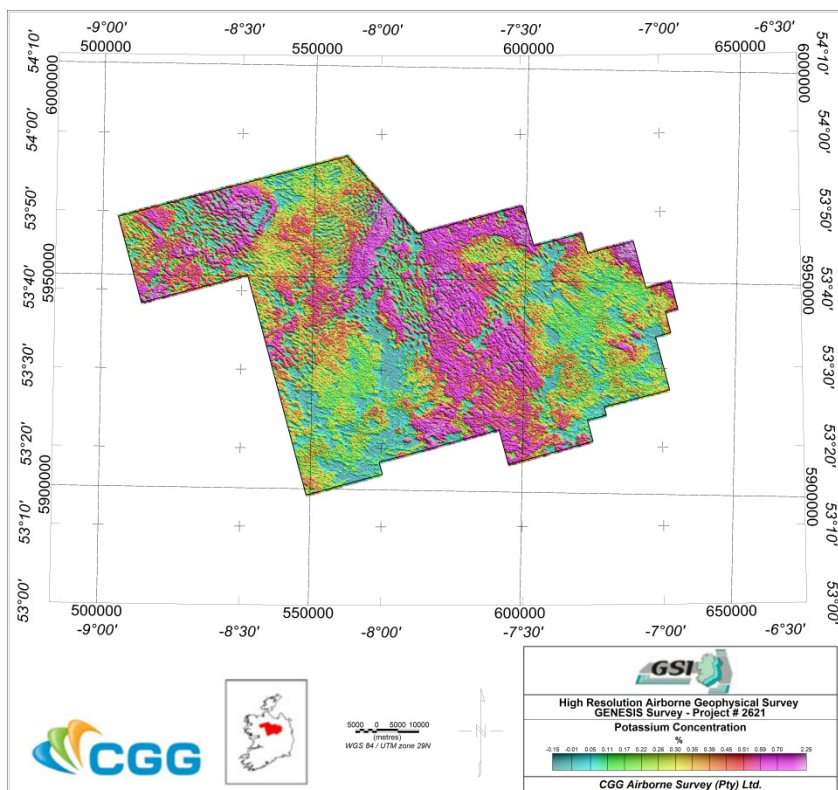


Figure 18: Tellus North Midlands – Potassium Concentration (Using 60m Height Correction)

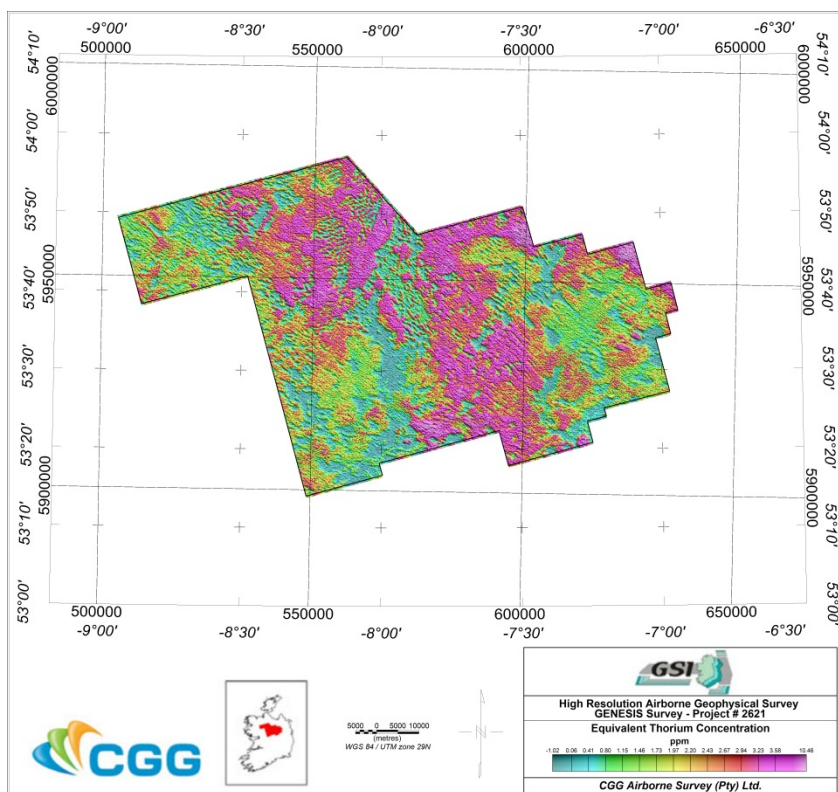


Figure 19: Tellus North Midlands – Equivalent Thorium Concentration (Using 60m Height Correction)

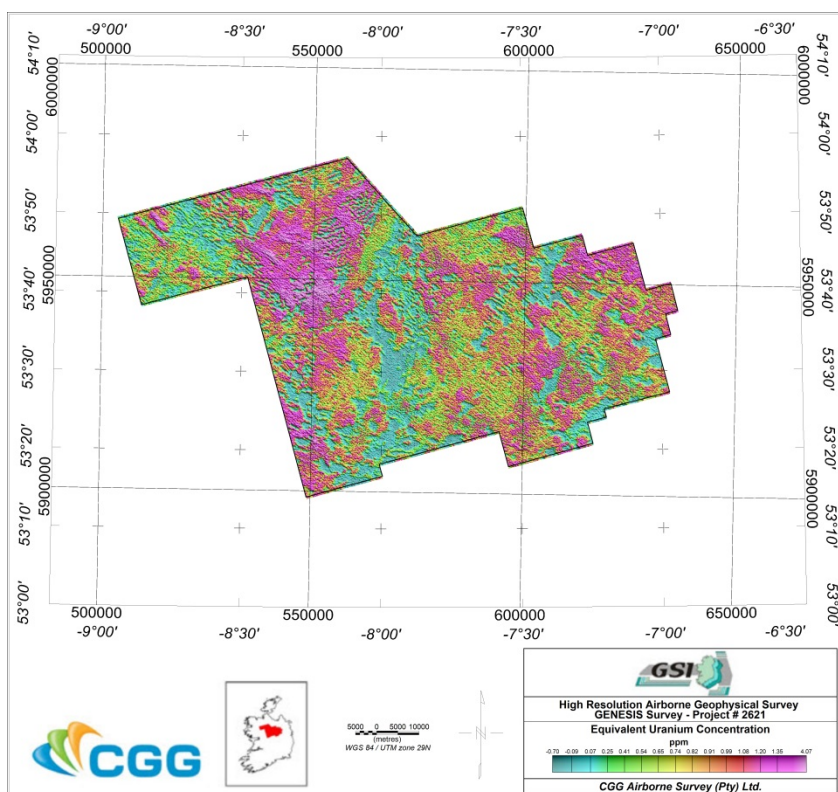


Figure 20: Tellus North Midlands – Equivalent Uranium Concentration (Using 60m Height Correction)

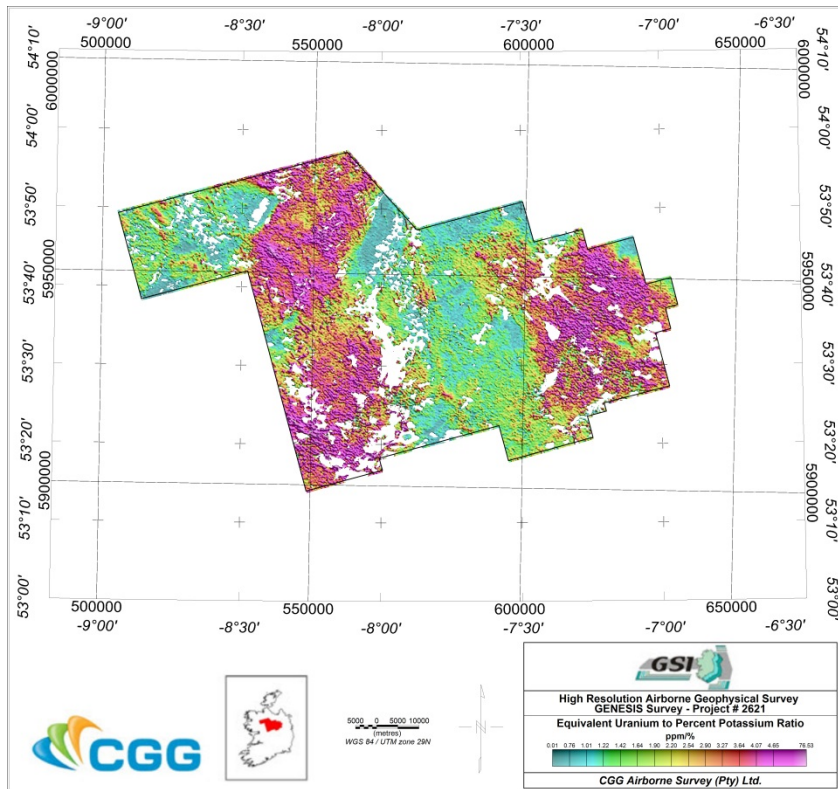


Figure 21: Tellus North Midlands – Equivalent Uranium to Percent Potassium Ratio (Using 60m Height Correction)

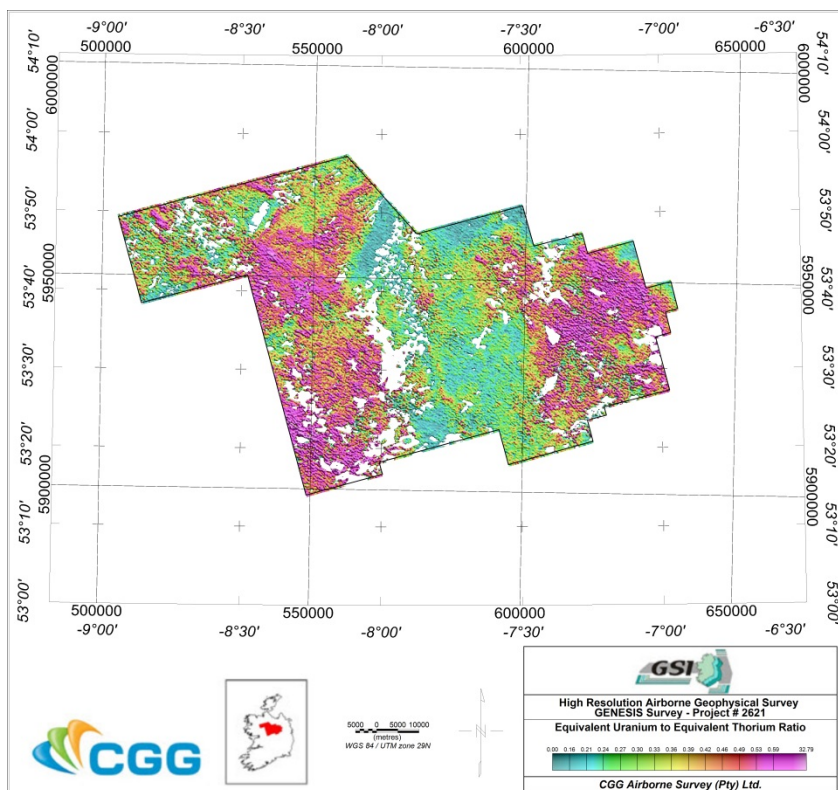


Figure 22: Tellus North Midlands – Equivalent Uranium to Equivalent Thorium Ratio (Using 60m Height Correction)

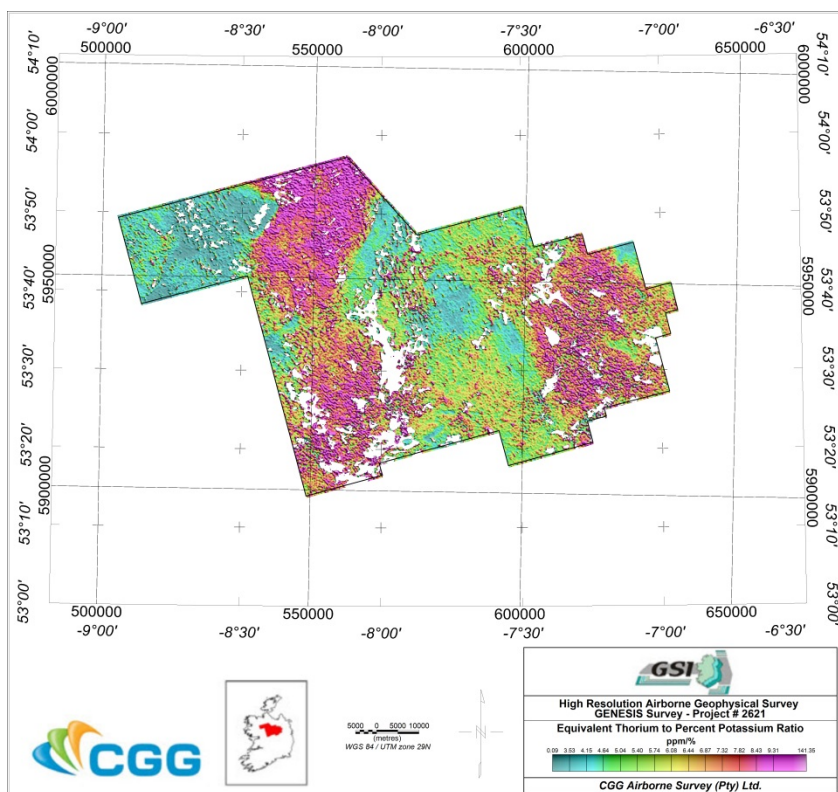


Figure 23: Tellus North Midlands – Equivalent Thorium to Percent Potassium Ratio (Using 60m Height Correction)

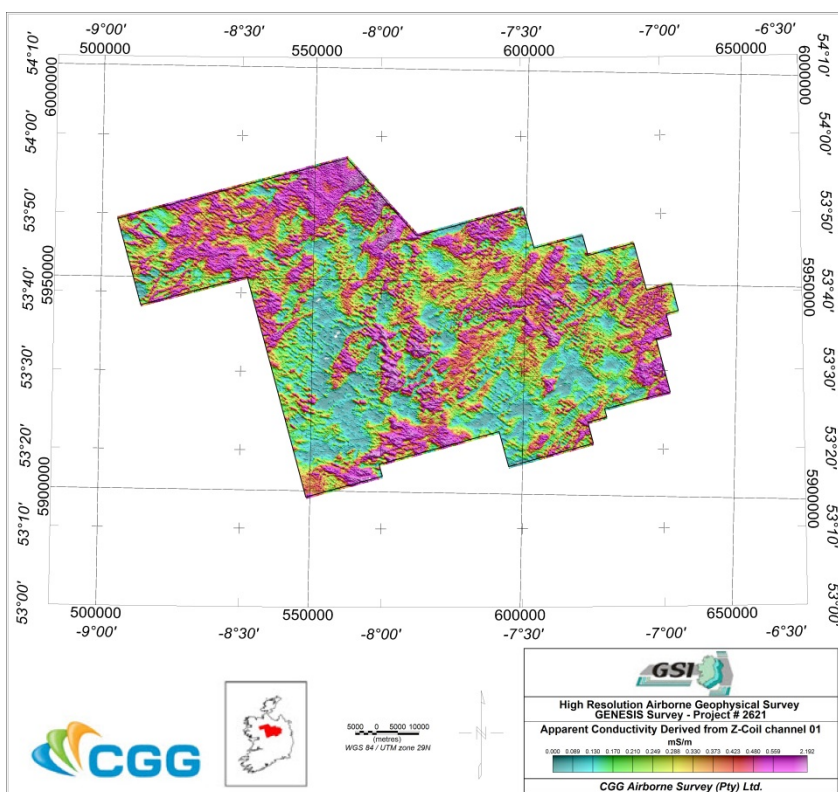


Figure 24: Tellus North Midlands – Apparent Conductivity Derived from Z-Coil channel 01

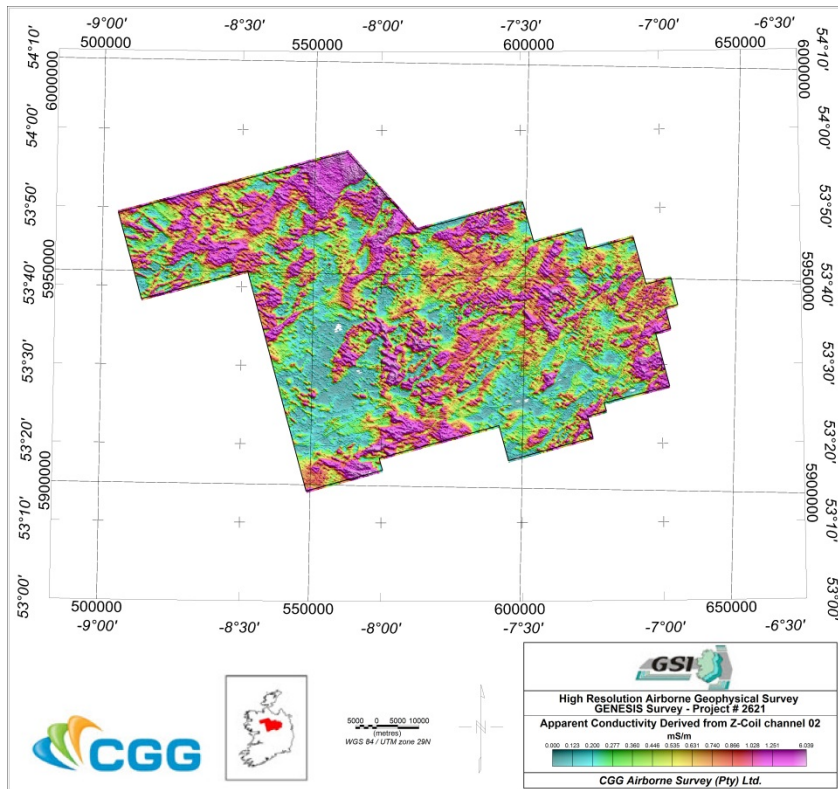


Figure 25: Tellus North Midlands – Apparent Conductivity Derived from Z-Coil channel 02

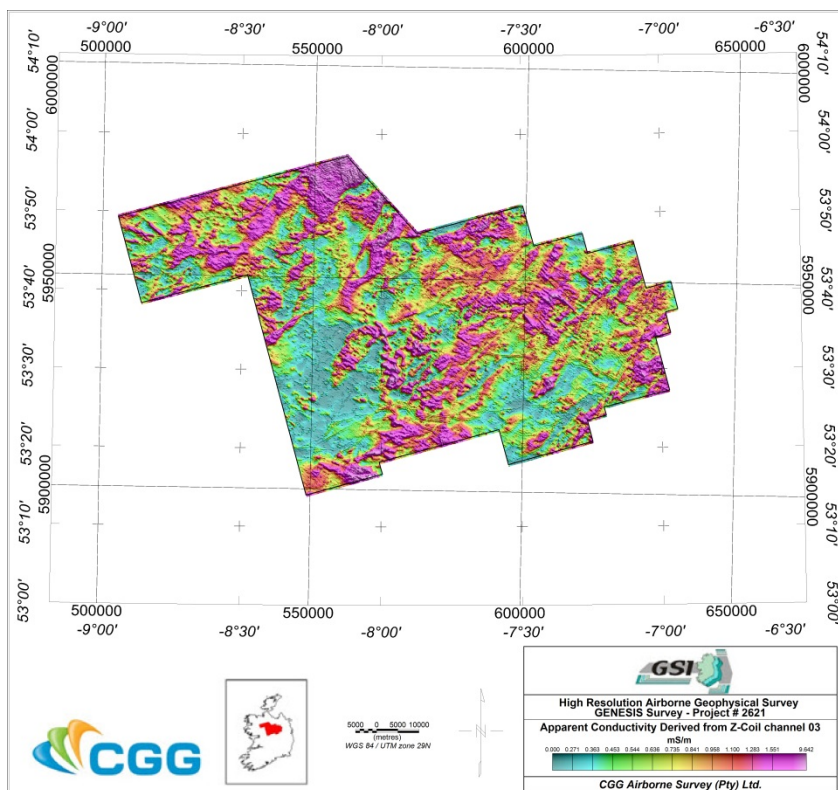


Figure 26: Tellus North Midlands – Apparent Conductivity Derived from Z-Coil channel 03

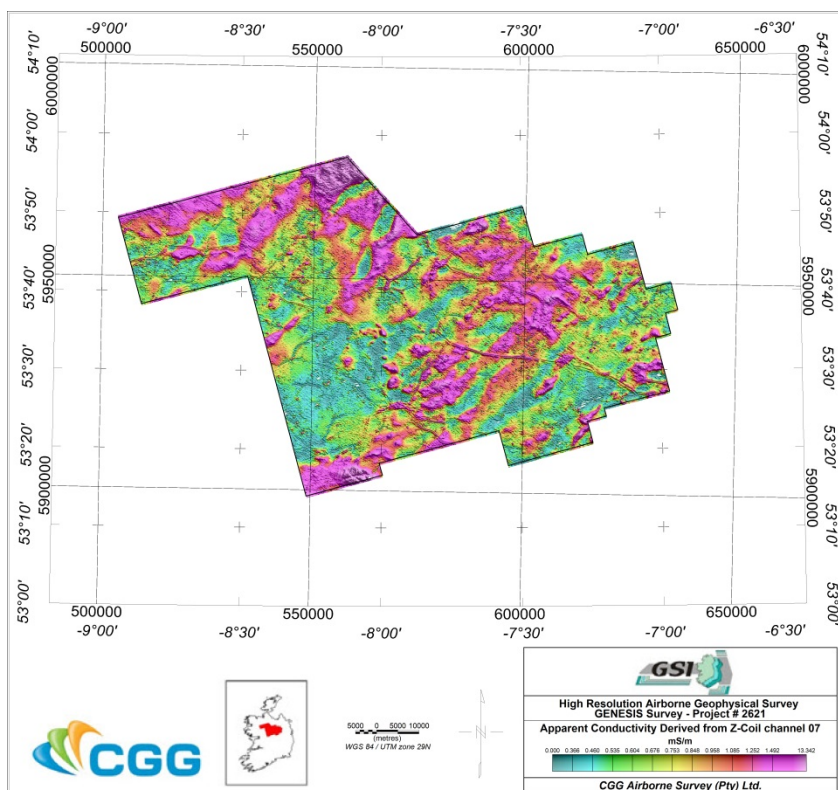


Figure 27: Tellus North Midlands – Apparent Conductivity Derived from Z-Coil channel 07

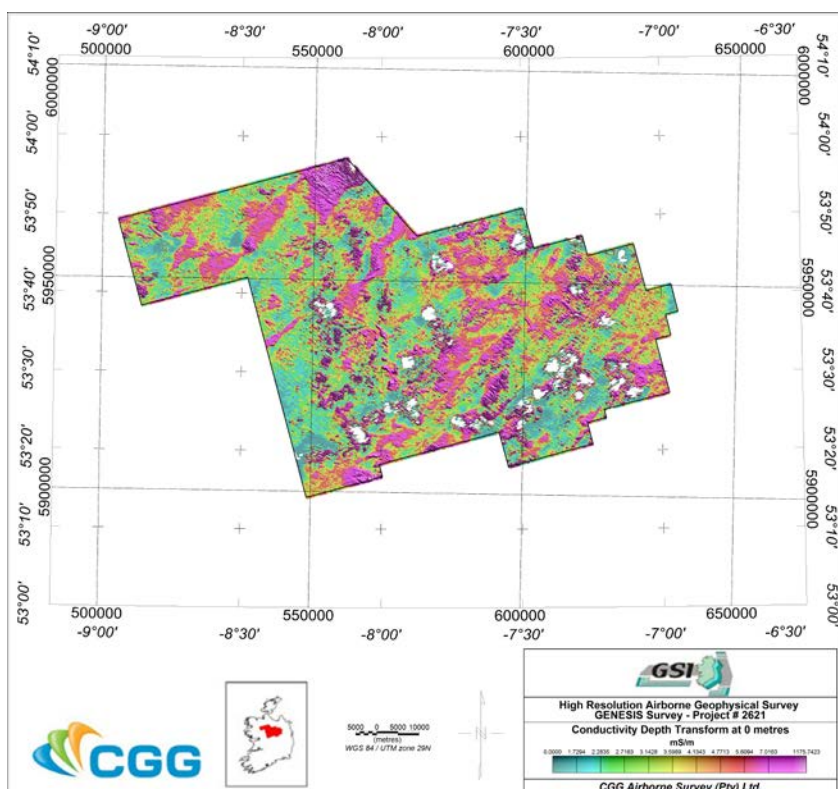


Figure 28: Tellus North Midlands – Conductivity Depth Transform at 0m

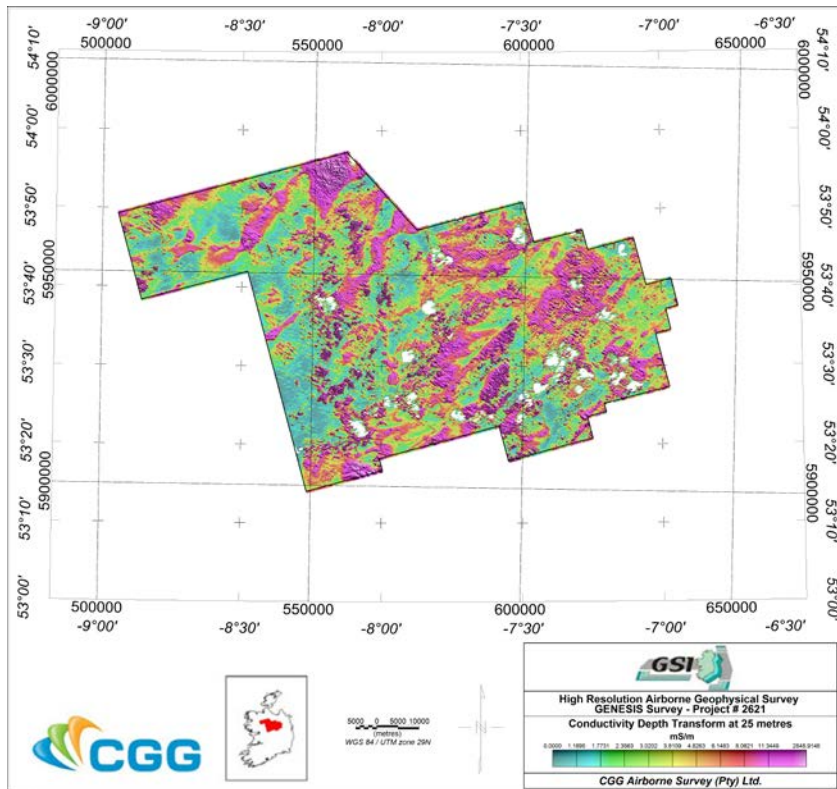


Figure 29: Tellus North Midlands – Conductivity Depth Transform at 25m

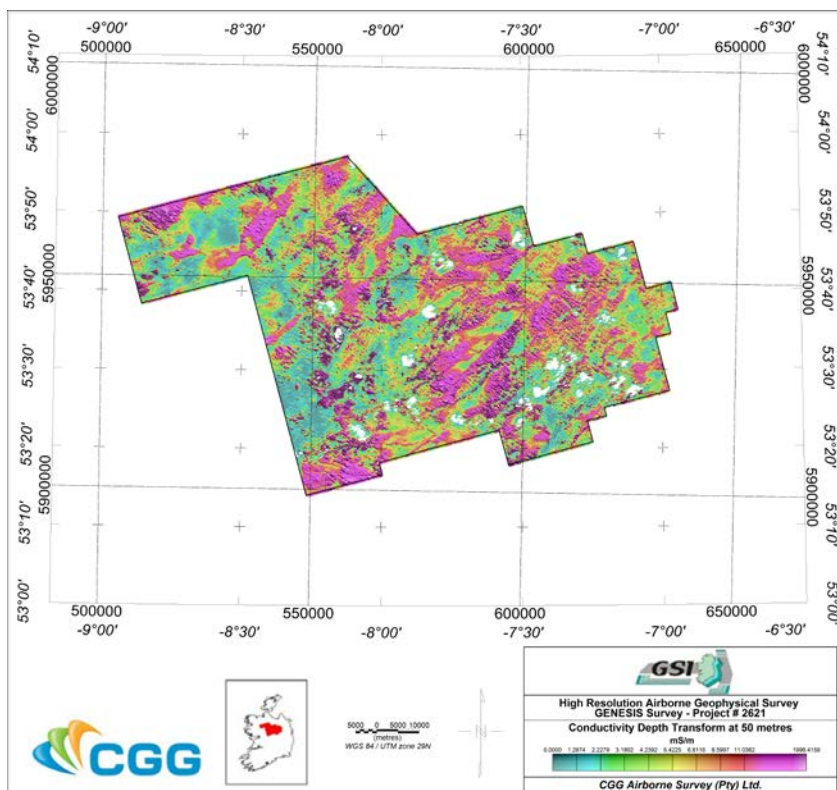


Figure 30: Tellus North Midlands – Conductivity Depth Transform at 50m

10 APPENDIX III – List of All Supplied Data

10.1 Preliminary Gridded Data

Preliminary gridded data were produced in Geosoft format

- Digital terrain model (m ASL)
- Total magnetic intensity (nT)
- Total Count (cps)
- Potassium (cps)
- Thorium (cps)
- Uranium (cps)
- Cesium (cps)

10.2 Final Located Data

0.2 second electromagnetic data

0.2 second conductivity depth transforms (CDT) data

0.1 second magnetics and digital terrain data

1.0 second windowed radiometrics data

1.0 second raw 256 channel radiometric data

1.0 second cesium radiometric data

Final located data are in Geosoft GDB / ASCII format. Contents of each are shown in Appendix II.

10.3 Final Gridded Data

Final gridded data were produced in Geosoft format.

- Digital Terrain Model (m MSL)
- Residual Magnetic Intensity (nT)
- Total magnetic intensity (nT)
- First Vertical Derivative of Total Magnetic Intensity (nT/m)
- Second Vertical Derivative of Total Magnetic Intensity (nT/m²)
- Calculated Lateral Gradient of Total Magnetic Intensity (nT/m)
- Calculated Longitudinal Gradient of Total Magnetic Intensity (nT/m)
- * Total Count (cps)
- * Potassium (cps)
- * Thorium (cps)
- * Uranium (cps)
- * Cesium (cps)
- * Total Count Air Absorbed Dose Rate (nGy/h)
- * Potassium Concentration (%)
- * Equivalent Thorium Concentration (ppm)
- * Equivalent Uranium Concentration (ppm)
- * Equivalent Uranium to Percent Potassium Ratio (ppm/%)
- * Equivalent Uranium to Equivalent Thorium Ratio
- * Equivalent Thorium to Percent Potassium Ratio (ppm/%)
- Apparent Conductivity Derived from Z-Coil channel 01
- Apparent Conductivity Derived from Z-Coil channel 02
- Apparent Conductivity Derived from Z-Coil channel 03
- Apparent Conductivity Derived from Z-Coil channel 04
- Apparent Conductivity Derived from Z-Coil channel 05
- Apparent Conductivity Derived from Z-Coil channel 06
- Apparent Conductivity Derived from Z-Coil channel 07
- Apparent Conductivity Derived from Z-Coil channel 08

- Apparent Conductivity Derived from Z-Coil channel 09
- Apparent Conductivity Derived from Z-Coil channel 10
- Apparent Conductivity Derived from Z-Coil channel 11
- Conductivity Depth Transform at 0m
- Conductivity Depth Transform at 25m
- Conductivity Depth Transform at 50m
- Conductivity Depth Transform at 75m
- Conductivity Depth Transform at 100m

* Note – Height corrected to both 60m and 90m

10.4 Additional Products

Logistics and Processing Report

Calibration Report for Aircraft VH-ZKB

Calibration Report for Aircraft VH-ZKG

Digital Video

Bundoran Test Line

11 APPENDIX IV – System Tests and Calibrations

Please refer to the following documents for detailed calibration results: Calibration Report for Aircraft VH-ZKB and Calibration Report for Aircraft VH-ZKG.

Flights not mentioned below were non-production flights, they either were system test flights, calibration flights, or production flights aborted.

11.1 Aircraft VH-ZKB (previously ZS-FSA)

11.1.1 Figure of Merit

- Flights 2 to 8 inclusive used FOM flown September 24th, 2014, port was 1.538 nT & starboard was 1.234 nT
- Flights 20 to 57 inclusive used FOM flown November 18th, 2014, port was 1.112 nT & starboard was 1.036 nT
- Flights 58 to 94 inclusive used FOM flown March 4th, 2015, port was 1.281 nT & starboard was 1.058 nT
- Flights 96 to 102 inclusive used FOM flown April 18th, 2015, port was 0.955 nT & starboard was 0.692 nT

11.1.2 Heading

- Flown November 18th, 2014, port difference was 2.42 nT & starboard difference was 1.62 nT

11.1.3 Altimeter Calibration

- Flights 2 to 8 inclusive used altimeter calibration flown October 1st, 2014, $\text{radar_linear} = -0.000112 * \text{ADC1_4} + 3.907915$
- Flight 20 inclusive used altimeter calibration flown October 20th, 2014, $\text{radar_linear} = -0.000122 * \text{ADC1_4} - 0.509755$
- Flights 23 to 102 inclusive used altimeter calibration flown November 11th, 2014, $\text{radar_linear} = -0.000117 * \text{ADC1_4} + 3.168645$

11.1.4 Lag and Parallax Control

- Flown on September 24th, 2014, electromagnetic lag was 2.8 sec. while magnetic port & starboard lag were 0.4 sec.

11.1.5 Pad Calibration

- Completed August 6th, 2014, refer to section 6.5.12 for results and Calibration Report for Aircraft VH-ZKB for more details.

11.1.6 Height Attenuation and Sensitivity Calibration

- Completed September 9th, 2014, refer to section 6.5.13 and 6.5.14 for results and Calibration Report for Aircraft VH-ZKB for more details.

11.1.7 Cosmic Test

- Completed April 10th, 2015, refer to section 6.5.9 for results and Calibration Report for Aircraft VH-ZKB for more details.

11.1.8 Radon Test

- Completed May 22nd, 2015, refer to section 6.5.11 for results and Calibration Report for Aircraft VH-ZKB for more details. (Results were combined from both VH-ZKB and VH-ZKG)

11.2 Aircraft VH-ZKG (previously ZS-SSA)

11.2.1 Figure of Merit

- Flights 506 to 522 inclusive used FOM flown October 4th, 2014, port was 0.930 nT & starboard was 0.821 nT.

- Flights 524 to 559 inclusive used FOM flown February 18th, 2015, port was 0.642 nT & starboard was 0.487 nT

11.2.2 Heading

- Flown October 4th, 2014, port difference was 3.55 nT & starboard difference was 1.31 nT

11.2.3 Altimeter Calibration

- Flights 506 to 559 inclusive used altimeter calibration flown October 6th, 2014, radar_linear = -0.000120*ADC1_4 +6.952430

11.2.4 Lag and Parallax Control

- Flown on October 14th, 2014, electromagnetic lag was 2.8 sec. while magnetic port & starboard lag was 0.3 sec.

11.2.5 Pad Calibration

- Completed August 6th, 2014, refer to section 6.5.12 for results and Calibration Report for Aircraft VH-ZKG for more details.

11.2.6 Height Attenuation and Sensitivity Calibration

- Completed September 9th, 2014, refer to section 6.5.13 and 6.5.14 for results and Calibration Report for Aircraft VH-ZKG for more details. (Height attenuation and sensitivity results were used from VH-ZKB)

11.2.7 Cosmic Test

- Completed April 21st, 2015, refer to section 6.5.9 for results and Calibration Report for Aircraft VH-ZKG for more details.

11.2.8 Radon Test

- Completed May 22nd, 2015, refer to section 6.5.11 for results and Calibration Report for Aircraft VH-ZKG for more details. (Results were combined from both VH-ZKB and VH-ZKG)